

Pulse Transit Time Measurement Method with Artifact Tolerance for Home Healthcare

Naoto Shiraishi

Graduate School of Systems and Information Engineering,
University of Tsukuba
1-1-1 Tennodai, Tsukuba, Ibaraki 305-8573, Japan
shiraishi@golem.kz.tsukuba.ac.jp

Yoshiyuki Sankai

Faculty of Engineering, Information and Systems
University of Tsukuba
1-1-1 Tennodai, Tsukuba, Ibaraki 305-8573, Japan
sankai@golem.kz.tsukuba.ac.jp

Abstract – To measure the arterial stiffness at home is important in order to prevent and treat arteriosclerosis. Pulse wave velocity (PWV) is one of the indexes of arterial stiffness. We have proposed a device that measures PWV at home. The device measures pulse transit time (PTT) and calculates PWV using the PTT. The PTT measurement is used electrocardiogram (ECG) and photoplethysmogram (PPTG). The operator of the device is user oneself. At home, it is difficult to judge whether the measurement condition is appropriate because medical staff is not at home. Motion artifacts are problem that occur as well. The method with artifact tolerance is useful for both increasing the measuring precision and decreasing re-measurement to suppress the motion artifact automatically. Therefore, the purpose of this research is to propose a pulse transit time measurement method with artifact tolerance, and to evaluate its measurement precision. We proposed the method that outlier of PTT is excluded using an average and a standard deviation (SD). The average and the SD are calculated using R-wave and peaks of PPTG in 30 seconds. An experiment that ECG or PPTG has deliberate motion artifacts was performed with developed measurement system. To evaluate, we used the developed measurement system that has the pulse transit time measurement method with artifact tolerance. Precision of the measurement system was 7.97% when ECG or PPTG with the artifact. It was smaller than 8.4% that is precision of the existing medical equipment. Therefore the proposal method that has sufficient artifact tolerance was confirmed.

Index Terms – arteriosclerosis, pulse wave velocity, pulse transit time, artifact tolerance

I. INTRODUCTION

In the world, cardiovascular diseases account for 31% of its mortality. Arteriosclerosis accounts for 78% of the cardiovascular diseases [1]. Blood pressure is checked at home in order to prevent and treat the cardiovascular diseases [2]. Because blood pressure is affected by not only atherosclerosis but also other factors, arteriosclerosis is not accurately known from blood pressure measurement [3]. In medical institutions, pulse wave velocity (PWV) is measured in order to inspect arterial stiffness [3-7]. Pulse transit time (PTT) is used to calculate PWV. PTT is measured with air plethysmogram or pressure pulse wave.

Home devices need precision at the same level as exiting devices and miniaturization. An air plethysmogram sensor and a pressure pulse wave sensor are difficult to miniaturize because these need an air compressor or attachments. Moreover Accurate positioning of these sensors are important

for precision. Our research group has proposed a measurement device of arteriosclerosis for measurement of hospital level [8-9]. The device measures electrocardiogram (ECG) and photoplethysmogram (PPTG) to calculate PWV. An ECG sensor and a PPTG sensor can be miniaturized because the sensors consist of only electronic circuits and the sensors don't need air compressor. The PWV measurement using ECG and PPTG has been reported [10-12], however feasibility of the PTT measurement has been shown using a general-purpose recorder in a condition without an artifact. The research only used the general-purpose recorder, and home equipment has never developed.

The device we proposed is measured with both electrodes attached to the chest and a photo sensor attached to the fingertip. Changes in condition of contact between the electrodes or the photo sensor and the skin cause motion artifacts. The artifacts cause a decrease in measurement precision. In medical institutions, when professionals such as doctors find the artifact, ECG and PPTG can be measured again. However, in the home, we cannot check the artifact and cannot measure again because the professionals are not in the home. In addition, repetition of measurement increases measurement time and effort. Therefore, to prevent repetition of measurement and a decrease in the precision of measurement, a method that reduces automatically the artifacts is necessary for the PTT measurement device. The PTT is influenced directly by the artifact, because the PWV is calculated using the PTT that is measured with ECG and PPTG.

Therefore, the purpose of this research is to propose a pulse transit time measurement method with artifact tolerance, and to evaluate its measurement precision.

II. DEVELOPMENT AND METHOD

A. Measurement of Pulse Transit Time

An artifact caused by contact failure of a measurement probe is not canceled in previous research that a measurement device requires users to keep motionless and measurements by medical specialists. We have been developed a personal and miniaturized measurement system for home healthcare that enables us to obtain PTT data without medical specialists. In order to calculate PTT The system uses to measure ECG with electrodes and to measure PPTG with an optical sensor.

Accurate PTT calculation requires synchronization between ECG and PPTG. The integration of the ECG and

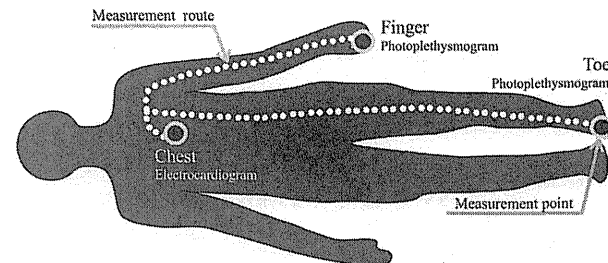


Fig. 1 Measurement points and measurement routes.

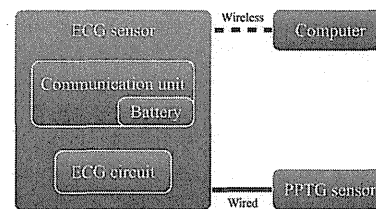


Fig. 2 The schematic diagram of the measurement system.

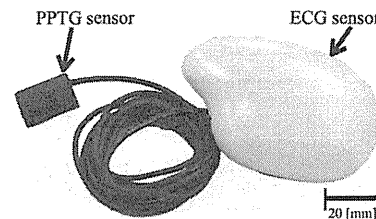


Fig. 3 Appearance of the measurement device.

PPTG sensors that are developed in previous study contributed to measure synchronized ECG and PPTG signals within 1 ms time lag.

PWV is an index to estimate arteriosclerosis development that reflects stiffness of a target vessel. The vessel is defined two points of arterial blood pressure measurement. Another target vessel is defined by other measurement points. Fig. 1 shows measurement points. In this research, two sets of measurement points are defined: measurement point set of the chest for ECG and a tip of a toe for pulse wave that is compatible to conventional measurement method; measurement point set of chest for ECG and finger tip for pulse wave that are easy to measure. Each target vessels

include an aorta that relates serious diseases. The target vessel between a tip of a toe and the chest includes leg artery that is one of the site of favorite site for arteriosclerosis obliterans. The target vessel between a fingertip and the chest includes arm artery.

B. Measurement System

Fig. 2 shows a structure of a measurement system. The system consists of a measurement device and a computer. Communication between the measurement device and the computer is wireless. The computer is installed software that controls the measurement device, calculates PTT and displays ECG, PPTG and PTT.

1) **Measurement device:** The measurement device is simple appearance (Fig. 3). The device is enough small to get hold and easy to use solely. The measurement device has two parts. One of the parts (96x60x21 mm) is ECG sensor. Another part (21x17x9 mm) is PPTG sensor. The device has only a toggle switch and is easy to use. The measurement procedure is automatic. The procedure starts by a click of a button on the software on the computer. Such simple operation is convenient to use for non-specialists at home healthcare. Users attach the pulse wave sensor to a finger or a toe and put the ECG sensor on a chest to utilize the device.

The pulse wave probe is wired to the communication unit. The communication unit supplies power to the pulse wave probe and receives signal from the probe. The wired connection makes the probe small by omitting power source and communication circuits.

The ECG sensor has communication unit and signal processing circuit for ECG measurement. The communication unit has a microcontroller, a wireless communication module and a battery. The microcontroller is dsPIC30F3013 (Microchip Technology Inc. U.S.A.). It has an analog/digital converter (12 bit, 1 kHz). The wireless communication module is KC22 (KC wirefree). It is a Bluetooth module. It guarantees enough communication speed and long communication distance. The module uses serial communication by serial port profile. The battery is lithium-ion rechargeable battery (3.7 V, 1000 mAh). It is power source of the measurement device. The battery is charged by USB and a charging circuit is in the unit.

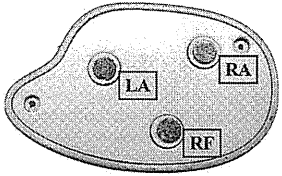


Fig. 4 The layout of the electrodes for electrocardiogram measurement

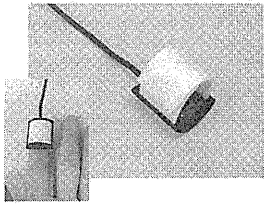


Fig. 5 The photoplethysmogram sensor and an example of fixing

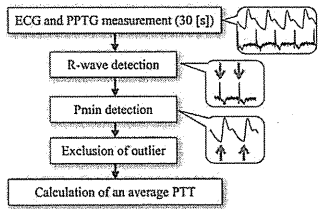


Fig. 6 Procedure of PTT calculation

The ECG is measured with three electrodes (diameter 8 mm) and the signal processing circuit. The electrodes are made of Ag-AgCl disk that is suitable for biological measurement. There are two electrodes for differential amplification, and there is an electrode for ground. Fig. 4 shows the layout of the electrodes. Waveforms measured by this sensor are similar to leads I that is one of the 12-leads ECG. Signals that are detected by the electrodes are amplified and filtered with the signal processing circuit.

The pulse wave probe has a light emitting diode (LED), a photodiode (PD) and a signal processing circuit. Pulse wave signals detected by the PD are amplified and filtered with the signal processing circuit. The wavelength of the LED is 940 nm. This wavelength is suitable for PPTG measurement because of high absorbance in blood and low absorbance in other tissue. Both the LED and the PD put on a same plane in order to attach. A hook-and-loop fastener as shown in Fig. 5 is used to fix the probe. In this way the probe can attach both finger and toe.

2) *Algorithm for Measurement of Pulse Transit Time:* Precision of PWV measurement is affected by PTT, because the length of blood vessels in adults is not changed. It is important to measure PTT with high precision. And it is necessary that the signal processing is simple in order to measure quickly. Therefore the following method is used in this study and the algorithm is in the software.

First, we explain a way to detect feature points of ECG and PPTG in order to calculate PTT. The PTT is defined as an average of time differences for 30 seconds between an R-wave of ECG and a leading edge of PPTG. The R-wave is defined a maximum point in one heartbeat. The leading edge of PPTG is defined a minimum point (P_{min}) in one heartbeat. Procedure of PTT calculation is R-wave detection, P_{min} detection, calculation of the time difference between R-wave and P_{min} , exclusion of outliers, calculation of an average PTT (Fig. 6). The ECG signals transmit to high pass filter. Its cut-off frequency is 0.1 Hz in order to reduce base-line drift before R-wave detection. The PPTG signals transmit to a moving average filter of 30 samples in order to reject high frequency noise before P_{min} detection. The PTT is calculated when the number of R-wave detection in heart rates equivalent is more than 40 beat per minute and less than 120 beat per minute. Because, it is considered that the electrodes or the PPTG sensor has a bad condition such as electrical contact.

Second, we explain an exclusion process of outliers for the measurement has the artifact tolerance. The PTT that is time difference between R-wave and P_{min} is calculated by (1).

$$T_{PTT} = t_P - t_R \quad (1)$$

Where, T_{PTT} is a PTT, t_R is time of R-wave, t_P is time of P_{min} , and t_R is smaller than t_P . The artifacts cause failure of detecting the feature point that is R-wave or the P_{min} . The failure of detection is that the feature point is undetectable or that the detected point is wrong. In this case, PTT is incorrect. The measurement that has artifact tolerance can be performed with exclusion of incorrect PTT. We propose the method that decides range of PTT dynamically.

A range of PTT is defined as a mean of time differences and a standard deviation (SD) of the time differences. The time differences are defined between R-wave and maximum point of PPTG in one heartbeat. The range of PTT is from the mean minus the SD to the mean plus the SD. The time differences that are out of the range are excluded. This exclusion process is repeated. When the SD is less than 3 % of the mean, the repetition of the process stops.

III. EXPERIMENTS

A. Detection of Feature Point

We conducted an experiment of detecting the feature points that are R-wave and P_{min} . Each feature point is detected in ECG or PPTG. In three subjects (healthy person, 22 to 28 years old), the measurement is performed with the developed device. The pulse wave probe is attached to a finger and a toe. In a subject, the measurement is one time each place. To inspect the detection, signals of the measurement that has non-artifact are adopted.

After resting for 5min, the measurement was performed in the supine position (Fig. 7). The pulse wave probe is attached to index finger of the left hand or big toe of left foot.

B. Evaluation of Fundamental Performance

We conducted a reproducibility experiment. In three subjects (healthy person, 22 to 28 years old), non-artifact signals are measured and the signal's coefficient of variance (CV) is calculated. Measurement points of PPTG are a fingertip and a tip of a toe in order to measure the vessels that are in an upper limb and lower limb.

The measurement is performed ten times for one subject. The sensor is attached each time. After resting for 5 minutes, the measurement was performed in the supine position. The PPTG sensor is attached a left fingertip or a tip of a left toe. The ECG sensor is attached a left chest.

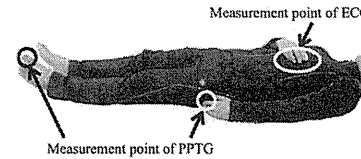
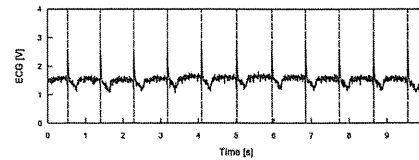
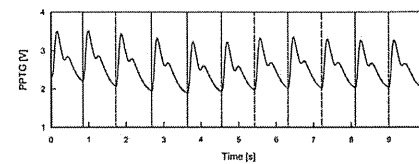


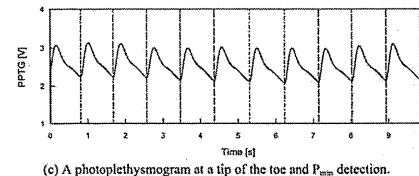
Fig. 7 The posture and points in the measurement



(a) An electrocardiogram and R-wave detection.



(b) A photoplethysmogram at fingertip and P_{min} detection.



(c) A photoplethysmogram at a tip of the toe and P_{min} detection.

Fig. 8 The examples of the result measurement of ECG or PPTG and detection of R-wave or P_{min} .

C. Evaluation of Artifact Tolerance

We conducted an experiment of motion artifact tolerance where the artifact is occurred deliberately. Measurement points of PPTG are a fingertip and a tip of a toe. This experiment compares two kind of PTT. The one of the PTT is calculated using the signals that have no artifact. It PTT is measured in (1) Detection of Feature Point. Another PTT is calculated using the signals that have artifact.

The effect of artifact in ECG and PPTG is inspected separately. The artifact in ECG is caused by contact failure of between the chest and the electrodes; accordingly the electrodes are separated from the chest in order to recreate the artifact. The artifact in PPTG is caused by change of contact situation of between the skin and the sensor; accordingly the sensor is shake at about 2-3 Hz in order to recreate the artifact.

In this experiment, we suppose that frequency of the artifact is 0 to 2 times in the 30 seconds measurement, when the subjects are instructed to rest. And the continuous artifact is not occurred. Therefore experiment condition is decided the frequency of the artifact is 3 times more than the supposition. And duration of the artifact is 1 second.

In three subjects (healthy person, 22 to 28 years old), four kinds of experiments are performed. Combinations of the experiment condition are upper or lower limb and the artifact in ECG or PPTG. The measurement is 5 times at one of the condition. A number of measurements in each condition are five times. After resting for 5min, the measurement was performed in the supine position. The pulse wave probe is attached to first finger of the left hand or big toe of left foot.

It is enough precision that the error of this measurement is less than 8.4 % because repeatability of existing medical equipment is 8.4 % [3].

IV. RESULTS

A. Detection of Feature Points

Fig. 8 shows one of the results. We defined the feature points of ECG and PPTG. R-wave is the feature point of ECG. P_{min} is the feature point of PPTG. In Fig. 8 (a), a solid line is ECG and broken lines are time of R-wave detection. In Fig. 8 (b) and (c), a solid line is PPTG and broken lines are time of P_{min} detection. As can be seen from Fig. 8, the feature points were detected. In other subject, also, the feature points were detected.

B. Evaluation of Fundamental Performance

Table 1 shows the measurement results that are precision without the artifact. When PPTG was measured at the fingertip, average of standard deviation (SD) was 2.98 ms and an average of coefficient of variation (CV) each subject was 1.70 %. When PPTG was measured at the fingertip, average of the SD was 8.38 ms and an average of CV each subject was 2.94 %. The upper limb's CV is smaller than the lower limb's CV.

C. Evaluation of Artifact Tolerance

Table 2 shows the results that are PTT and errors. The error rate was calculated by (2), where E_r is the percent error rate, t_A is PTT with artifact, t_N is PTT without artifact.

$$E_r = 100 (t_A - t_N) / t_N \quad (2)$$

The maximum error rate was -7.96 % each measurement part and each subject. The maximum error rate of each measurement parts was 3.53 % when PPTG was measured by fingertip and PPTG has artifact. The absolute value of (2) of each subject was used in order to calculate the maximum error rate.

V. DISCUSSION

From the result of detection of the feature point, when the signals have no motion artifact, we made sure that detection of the feature point was performed properly. The detection was performed properly regardless of subjects and the PPTG measurement point that is a finger or a toe.

From the result of evaluation of fundamental performance, the maximum CV was 2.94 % when the signals have no motion artifact. The PPTG measurement point of this result is toe. This result is smaller than 8.4 % that is repeatability of baPWV [3]. The target vessels of our device are similar to baPWV that is existing index of arteriosclerosis for medical institutions. The value of baPWV is result of the experiment of interobserver reproducibility. In our research, subjects attach the measurement device to own body and operate the measurement system. Because of this, experiment condition is not completely same as the experiment condition of baPWV. Our experiment only re-attaches the device on each measurement. The installation error and interobserver error are effect on interobserver reproducibility. Unlike the medical equipment used in medical institutions, an observer of our device and a subject of our device are the same person. Therefore, considering that condition of use our device, we think that the comparison of the installation error of our device with reproducibility of baPWV is valid. In the case that the signals don't contain the motion artifact, the precision of our measurement system is sufficient. Because the installation error of our system is sufficiently smaller than the reproducibility of baPWV.

From the result of artifact tolerance, the precision of the measurement system is lower than the reproducibility of baPWV when the signals have the motion artifacts. Therefore, the measurement system has the artifact tolerance.

In this research, measurement points were a fingertip or a tip of a toe. In the evaluation of fundamental performance, CV

of the PTT that was measured on a fingertip was smaller than CV of the PTT that was measured on a tip of a toe. These were 1.70 % and 2.96 %. It is inferred from this result that measurement on the fingertip is more precision than measurement on the tip of a toe. It is thought that measurement on the fingertip is high convenience. It is more useful to measure PTT on the fingertip than to measure PTT on the tip of a toe for home health care. However, in the future, it is necessary to consider that statistically significant difference of the precision because the number of our experiments subjects is few. In addition, it is necessary to consider relationship to arteriosclerosis.

We used standard deviation and average in order to exclude of outlier. As other method, there is a way the range of PTT is defined in advance. The value of PTT depends on measurement point, height and arterial stiffness. Because of this, the range needs to be broad. However the broad range decreases the precision. Therefore, advance decision of a range is difficult.

VI. CONCLUSION

In this research, we proposed a pulse transit time measurement method with artifact tolerance, and evaluated its measurement precision. To evaluate the measurement precision, we used the developed measurement system that has the pulse transit time measurement method with artifact tolerance. Precision of the measurement system was 7.97% when ECG or PPTG has the artifact. It was smaller than 8.4% that is precision of the existing medical equipment. Therefore the proposal method that has sufficient artifact tolerance was confirmed.

TABLE I
THE RESULT OF PTT MEASUREMENT WITHOUT THE ARTIFACT

Subjects	Fingertip measurement			Tip of toe measurement		
	Mean ms	SD ms	CV %	Mean ms	SD ms	CV %
A	172.4	2.97	1.72	290.3	5.17	1.78
B	159.5	2.87	1.80	263.4	10.76	4.08
C	198.7	3.11	1.56	311.3	9.22	2.96
Mean	176.9	2.98	1.70	288.4	8.38	2.94

TABLE II
THE RESULT OF PTT MEASUREMENT WITH THE ARTIFACT

Subjects	Measurement point is the fingertip						Measurement point is tip of the toe							
	PTT without artifact ms	Artifact in ECG			Artifact in PPTG			PTT without artifact ms	Artifact in ECG			Artifact in PPTG		
		PTT ms	Error ms	Error %	PTT ms	Error ms	Error %		PTT ms	Error ms	Error %	PTT ms	Error ms	Error %
A	172.4	174.2	1.83	1.06	170.3	-2.03	1.18	290.3	296.8	6.50	2.24	295.2	4.86	1.67
B	159.5	157.0	-2.56	1.60	152.4	-7.14	4.48	263.4	265.9	2.51	0.95	242.4	-20.97	7.96
C	198.7	188.1	-10.5	5.29	188.9	-9.79	4.93	311.3	309.1	-2.20	0.71	308.0	-3.38	1.09
Mean	-	-	-	2.65	-	-	3.53	-	-	-	1.30	-	-	3.57

ACKNOWLEDGMENT

This study was supported by the "Center for Cybernetics Research (CCR) - World Leading Human-Assistive Technology Supporting a Long-Lived and Healthy Society" granted through the "Funding Program for World-Leading Innovative R&D on Science and Technology (FIRST Program)," initiated by the Council for Science and Technology Policy (CSTP).

REFERENCES

- [1] M. Shanthi, P. Puska, and B. Norrving, Global atlas on cardiovascular disease prevention and control. World Health Organization, 2011.
- [2] Mancia, Giuseppe, et al, "2007 Guidelines for the management of arterial hypertension The Task Force for the Management of Arterial Hypertension of the European Society of Hypertension (ESH) and of the European Society of Cardiology (ESC)," European heart journal, vol. 28, no. 12, pp. 1462-1536, 2007.
- [3] Y. Akira, et al, "Validity, reproducibility, and clinical significance of noninvasive brachial-ankle pulse wave velocity measurement," Hypertension Research, vol. 25, no. 3 pp. 359-364, 2002.
- [4] S. Jun., et al, "Brachial-ankle pulse wave velocity: an index of central arterial stiffness?," Journal of human hypertension, vol. 19 no. 5, pp. 401-406, 2005.
- [5] T. Hirofumi, et al, "Comparison between carotid-femoral and brachial-ankle pulse wave velocity as measures of arterial stiffness," Journal of hypertension, vol. 27, no. 10, pp. 2022-2027, 2009.
- [6] Y. Tomoyuki, et al, "Brachio-ankle pulse wave velocity and cardio-ankle vascular index (CAVI)," Biomedicine & pharmacotherapy, vol. 58, pp. S95-S98, 2004.
- [7] B. Jacques, et al, "Aortic pulse wave velocity as a marker of cardiovascular risk in hypertensive patients," Hypertension, vol. 33, no.5, pp. 1111-1117, 1999.
- [8] S. Tsujimura, et al, "Design and Implementation of Web-Based Healthcare Management System for Home Healthcare", 13th International Conference on Biomedical Engineering, pp. 1098-1101, 2008
- [9] F. Ichihashi, Y. Sankai, "Development of a portable vital sensing system for home telemedicine", Proc. of the 29th Annual International Conference of the IEEE Engineering in Medicine and Biology Society, pp. 5872-5877, 2007.
- [10] L. An-Bang, et al, "Measuring pulse wave velocity using ECG and photoplethysmography," Journal of medical systems, vol. 35, no. 5, pp.771-777, 2011.
- [11] M. Nizan, B. Khanokh, and Y. Slovik, "The difference in pulse transit time to the toe and finger measured by photoplethysmography," Physiological measurement, vol. 23, no. 1, p. 85, 2002.
- [12] L. Stavros, et al, "Validation of a device to measure arterial pulse wave velocity by a photoplethysmographic method," Physiological measurement, vol. 23, no. 3, p. 581, 2002.

The Discriminant Criteria Detecting Operational Intention from Myoelectricity for Alternative Interface System

Junji Takahashi^{1,✉}, Noel Segura Meraz², Yasuhisa Hasegawa³, and Yoshiyuki Sankai³

Abstract: This paper proposes an alternative interface system with novel architecture flexible enough to adapt to various types of physically challenged person and able-bodied person, and also capable of connecting to various devices, using a tablet computer as a central system with which a user are interacting. For this interface system surface myoelectricity of various muscles which a user still has control, are used as input signals for controlling a tablet. The aim of this system is to extract operational intention of user while user doing deskwork. The special patterns of myoelectric signals, which are rarely observed in daily life, are utilized for discriminating operational intention from motional intention. We developed discriminant criteria and validated it experimentally. Additionally the operability of our proposed interface system is evaluated by Fitts' law based test GUI. The experimental results show that our proposed system is better than other types of alternative interface system.

Keywords: myoelectric signal, Human-Computer interface, detecting human intention

1. INTRODUCTION

Interface technologies have been taking an important role in robotics research field to couple a human and an artifact, which has been becoming increasingly complex and more diversified. One of primary roles of interface device is to extract human intentions and transmit them to a device, such as a personal computer, a robotic manipulator, a power-operated vehicle, an automobile, and so on. A good interface device requires assurance, readiness and ease of learning. From this perspective, almost all interface devices for healthy person are designed under the assumption that they are inputted by fingers or hands. Recently, since the most deskwork is done with a laptop or desktop computer connecting with web, most business can be handled if only the function of the finger is available.

This study was supported by the "Center for Cybernetics Research (CCR) - World Leading Human-Assistive Technology Supporting a Long-Lived and Healthy Society" granted through the "Funding Program for World-Leading Innovative R&D on Science and Technology (FIRST Program)," initiated by the Council for Science and Technology Policy (CSTP), and also supported in part by the Global COE Program on "Cybernetics: Fusion of Human, Machine, and Information Systems" of University of Tsukuba.

¹Junji Takahashi, Department of Micro-nano Systems Engineering, Nagoya University (takahashi@robo.mein.nagoya-u.ac.jp), formerly University of Tsukuba.

²Noel Segura Meraz, Graduate School of Systems and Information Engineering, University of Tsukuba.

³Yasuhisa Hasegawa and Yoshiyuki Sankai, Center for Cybernetics Research, University of Tsukuba.

RECEIVED: 23, NOV., 2012; REVISED: 30, JAN., 2013; ACCEPTED: 30, JAN., 2013; PUBLISHED: 31, JAN., 2013.

ISSN: 2345-234X



010201001300192013000108

However, there is a people who do not have the function of finger due to various reasons; both-arms amputee, spinal cord injury, muscle dystrophy, and paralysis. They need an alternative interface system to control devices. The ultimate alternative interface system is a Brain-Machine interface (BMI) [1-2] which detects instantaneously intentions generated in the brain. Although the BMI is beneficial for patients with server paralysis in order to output their intention, it is difficult for the system to extract particular intention from near-infrared spectroscopy (NIRS) or electroencephalogram (EEG), because wide variety of intentions are generated and evaporating without stopping in human brain. The difficulty of discriminating intentions requires patients to train a lot so as to make full use of the BMI system.

On the other hand, because myoelectric signals can be registered on peripheral part of body after the intentions are separated off in a way, users do not have to practice the myoelectricity based interface system as hard as when they practice BMI system. The advantage of myoelectricity (easy to output user intention), has been recognized for a long time and studied for extracting motional intentions of user to control functional electric prosthetics [3-4] and powered exoskeletal assistive robot systems [5-6]. Englehart et al. has developed a classification scheme for multifunction myoelectric control [7-9]. They studied and founded a feature extraction method from myoelectric signals that the performance of it is either equaling or surpassing to frequency-domain features. Hence, most of the studies about motion classification from myoelectric signal utilize their methods. The feature extraction method and several classification methods are described in detail in [9]. Yokoi et al. have developed a tactile feedback system and integrated with their proposed prosthetic hands system for giving the amputee user tactile impressions [10]. Their system enhanced the mutual adaptation mechanism in user brain so as to learn easier. Sankai et al. have developed powered exoskeleton system named "HAL" for amplifying, assisting, and supporting motor ability of lower limb disabilities [9].

These studies utilize the myoelectric signal for detecting motional intentions to support user's own body part by exoskeletal limb or an alternative part such as prosthetic. On the contrary, we aim to utilize the myoelectric signals for detecting operation intentions to control an electric device. Therefore, the usage of myoelectricity of our proposed system is different from other studies. The pilot study has reported in [11], but the validation was not enough. In this paper, we reformulate the discrimination criteria and validate it experimentally.

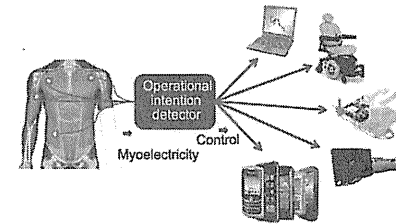


Fig. 1. Concept of the alternative interface system

In section 2, the myoelectric signal based interface system including the concept idea, electrode positions, calculation method, and the correspondence between muscles and cursor movements are described. Section 3 formulates the discriminant criteria between operational intention and motional intention from myoelectric signal. In section 4, the Fitts' law based performance test and the significant results of the test are described. Section 5 concludes the paper and sketches future research direction.

2. ALTERNATIVE INTERFACE SYSTEM USING MYOELECTRIC SIGNAL

A. Motivation and Concept

The myoelectricity induces muscles to contract. The contractile strength of muscle is roughly proportional to the amplitude and frequency of myoelectricity. However, there is no guarantee that same myoelectric signal patterns are always registered, even if a person remains fixed posture or takes same motions. This fact makes it difficult to extrapolate an actual intention from the myoelectric signal pattern in an accurate fashion. However, it can be said that a person is able to output various myoelectric signal patterns while he/she is taking a similar posture or motion. We regard this character of myoelectricity as an advantage and aim to develop a novel interface system which extracts operational intention separately from usual motions of body in order to control electric devices like a tablet (Fig. 1).

Considering the use of a computer, especially in the functional aspect, amputee does not need the prosthetic hand similar to real hand in appearance. Moreover, if only there is a transmitter which conveys operational intentions of the user to a computer accurately and smoothly, a physical hand is not needed for cursor control and keyboard input. Therefore, if only operational intentions can be picked up from some sort of his/her biological signal, an amputee or an upper limb disorder can use a computer. The purpose of this research is to develop an alternative computer interface between a person who has a dysfunction in both hands and a computer with using myoelectric signals from residual muscles of him/her. If this system is materialized, it promotes social reintegration of various types of physically challenged persons.

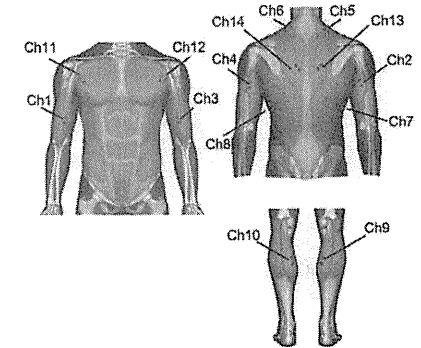


Fig. 2. The position of electrodes

TABLE I
CORRESPONDENCE BETWEEN CHANNELS AND MUSCLES

ch	muscle	ch	muscle
ch1	Right biceps brachii	ch9	Right triceps surae
ch2	Right triceps brachii	ch10	Left triceps surae
ch3	Left biceps brachii	ch11	Right pectoralis major
ch4	Left triceps brachii	ch12	Left pectoralis major
ch5	Right upside trapezius	ch13	Right middle trapezius
ch6	Left upside trapezius	ch14	Left middle trapezius
ch7	Right latissimus dorsi		
ch8	Left latissimus dorsi		

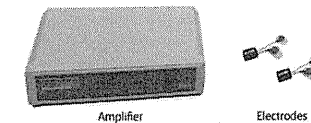


Fig. 3. ZeroWire EMG developed by AURION SRL: The electrodes send registered data to amplifier via wireless protocol.

B. Measurement of Myoelectric Signals from Various Muscles

Our approach is to register surface myoelectric signals from electrodes attached on the surface skin at various muscles. We investigated the ease of outputting the myoelectric signal at 14 numbers of muscles. The electrode positions and muscles corresponding with them are shown in Fig. 2 and Table 1. The diameter of each electrode and the centres distance between pair of electrodes are 14 mm and 30 mm, respectively.

The measurement system named ZeroWire EMG (Fig. 3), which consists of electrodes and amplifier device, utilized for experiments are shown in Fig. 3. The sampling frequency is 2000 Hz and 10-1000 Hz band pass filter are applied before the time series data are transmitted to the PC. According to the device manual, the time delay from the electrode to the PC is 20ms. Let $E(t)$ denote the data received at the PC for in

each instant of time t , T denote integral time and m denote channel number, then the integrated myoelectric signal $iE(t)$ for smoothing is defined as follows,

$$iE^m(t) = \frac{1}{T} \int_{t-T}^t |E^m(\tau)| d\tau. \quad (1)$$

Then the $iE(t)$ is normalized with Percent Maximum Voluntary Contraction (%MVC) method in order to compare the contraction level of different muscles, different subjects, and different days of experiment. The value of MVC^m is registered in every experiment. A subject is asked to contract the indicated muscles (m) for 2 seconds. Then the MVC^m is given from the registered data by follows equation,

$$MVC^m = \max_{0 \leq t \leq 2} \frac{1}{T} \int_{t-T}^t |E^m(\tau)| d\tau. \quad (2)$$

Finally, a normalized integrated myoelectric signal $nE(t)$ is given as follows,

$$nE^m(t) = \frac{iE^m(t)}{MVC^m} \times 100 \quad [\%]. \quad (3)$$

C. Correspondence between Muscles and Cursor Actions

The requirements of good interface device are that a user is able to manage it intuitively and that a user can become accustomed to the usage of it at once. Aiming this, manageable muscles are experimentally explored to decide the correspondence between muscles and cursor actions. A subject was asked to contract each muscle intentionally in turn to output myoelectric signal. Saying from the conclusion, the subject was able to output the signals from all muscles. However, a subject felt difficulty to output myoelectric signal at the both side of middle trapezius (ch13, 14) without contracting other muscles. Besides at the left side pectoralis major (ch11), the electro-cardiac potential (ECP) were registered strongly and involuntary. Thus these muscles should be excluded from the use for the interface.

TABLE 2
CORRESPONDENCE BETWEEN THE MUSCLE AND THE CURSOR ACTION

Cursor Action	Channels Muscles
Move to right	ch1, ch2 Biceps and triceps of right side
Move to left	ch3, ch4 Biceps and triceps of left side
Move to up	ch5, ch6 Right trapezius and left trapezius
Move to down	ch7, ch8 Right latissimus and left latissimus
Left click	ch10 Left triceps surae

Considering the control of a mouse cursor, 5 isolated signals are enough (right, left, up, down and click). So we decided to use the muscles, biceps brachii and triceps brachii, for right and left movement; trapezius upside muscles, for up movement; latissimus dorsi muscles, for down movement; triceps surae muscles, for click action, as shown in Table 2. Then we organized the interface in such a way that: the

mouse cursor takes action, when the registered $nE^m(t)$ of either channel exceeds a threshold k . However, this is not sufficient, because the cursor may take actions with usual body movements despite user's intention, and also because the body moves together with cursor movements. So, we developed discriminant criteria between operational intention and motional intention.

3. THE DISCRIMINANT CRITERIA BETWEEN OPERATIONAL INTENTION AND MOTIONAL INTENTION

A. Operational Intention and Motional Intention

A sequence of motions of human in daily life is realized by compositional contractions of extremities muscles or trunk muscles, and is rarely realized by a contraction of an isolate muscle. Meanwhile, we can contract an isolate muscle intentionally like a body builder without change our postures. These facts give us significant hint to design the discriminant criteria. Basically, we can design the discriminant criteria that the system detects operational intention when special myoelectric signal patterns, which are rarely registered in daily life, are registered. Wherein, we define an operational intention as a special pattern of myoelectric signals. And any other patterns of myoelectric signals are defined as motional intention.

B. The Special Patterns of Myoelectric Signals for Discriminating Operational Intention

In order to design an intuitive, easy-to-use, dependable interface system, the special patterns of myoelectric signal for outputting operational intentions should meet follows requirements,

- Requirement I:** A user can output the operational intention easily and can control a mouse cursor intuitively,
- Requirement II:** The operational intention should be detected without changing body posture or body motion trajectory,
- Requirement III:** The operational intention should not be detected when a subject takes usual motions in order to avoid false operation of mouse cursor.

In the section 2B, the correspondence between muscles and cursor actions are already derived from viewpoints of easiness and intuitiveness for cursor control as shown in Table 2. In this table, the cursor movements of right-and-left are assigned with biceps and triceps of each side. They are in relation of agonist-antagonist muscles of an elbow joint. The joint angle is determined by a total strength of these muscles contraction. From the perspective of the energy efficiency, the agonist-antagonist muscles rarely contract simultaneously in daily life. Briefly, the simultaneous contraction of the agonist-antagonist muscles is one of the special patterns of myoelectric signal. So, this combination fulfils the *Requirement III*. Moreover, we can contract these muscles with same tension so as not to change the elbow

angle. This meets the *Requirement II*.

The cursor up movement is assigned with right and left trapezius. The simultaneous contraction of them is often observed when a user holds up something with one's hands, but besides that, it is not often observed. So, the *Requirement III* is roughly satisfied as long as a user is careful about it. The cursor down movement is assigned with right and left latissimus. The simultaneous contraction of them is rarely observed unless a user does chin-up. So, the *Requirement III* is satisfied.

Because the both side trapezius and the both side latissimus are not in relation of agonist-antagonist muscles, body movements arise. However the body movements are not so large to affect the one's posture. So, it can be considered that the *Requirement III* is satisfied.

The click action is assigned with left triceps surae. In this study, it is assumed that a user control a PC with sitting on a chair or lying in a reclining chair. So, the legs are free and *Requirement II* and *III* are satisfied.

The condition that the system detects an operational intention is simultaneous contraction of combination muscles defined above. It means the pair of normalized integrated myoelectric signals exceeds the threshold and defined mathematically as follows,

$$\begin{cases} \text{Action on} : & k \leq nE^m(t), nE^{m+1}(t) \\ \text{Action off} : & \text{others.} \end{cases} \quad (4)$$

C. Experimental Evaluation of Discriminant Criteria

1) *Experimental Condition:* The purpose of this experiment is to confirm that the selected muscles combinations meet the Requirement I, II, and III. The test was conducted in two sessions for each muscles combination by a subject sitting on a chair. In the first session, a subject is asked to rhythmically contract each muscles combination five times and then keep contraction of it for 5 seconds. They are for checks of responsiveness and continuousness. In the second session, a subject takes usual motions likely to confuse the system; arranging a bookshelf, tidying up a desk, lifting a notebook computer by both hands, picking a pen up from the floor. This session is for check how much the system satisfies the Requirements III. The integral time T is 100 [ms] and the threshold k is 15 [%MVC] in all test.

2) *Experimental Results:* The experimental results of all muscle combinations are shown in Fig. 4. In the left side graphs, which are results of first session of each muscles combination, it is confirmed that the system correctly detects user's operational intention. In the right side graph, it is confirmed that the system is not confused by usual motions. However, in the case that the subject lifts a notebook computer by both hands, the system wrongly detects operational intention (Fig. 5). So, a user is expected not to lift something with both hands, when he/she uses the proposed alternative interface system. Nevertheless, it can be said that the proposed discriminant criteria meets the Requirements described in section 3B.

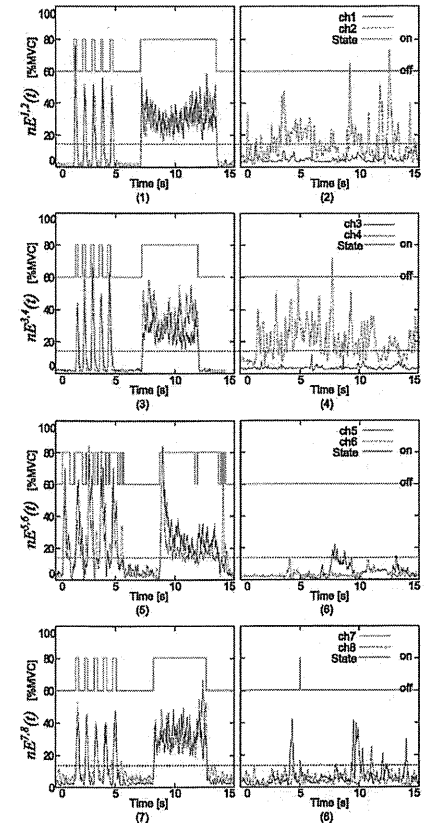


Fig. 4. Experimental results: The right sides are second sessions; (2) and (4) are the case of arranging a bookshelf, (6) is the case of tidying up a desk, (8) is the case of picking a pen up from the floor.

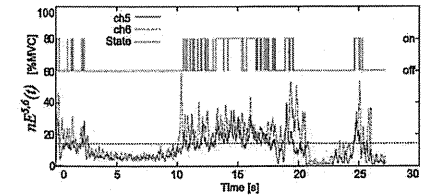


Fig. 5. One of the typical results of that the system wrongly detects the operational intention. At the beginning, during from 10s to 20s, and around 25s, the subject lifts the notebook computer with his both hand.

4. OPERABILITY TEST

A. Fitts' law based operability test

So as to evaluate the performance of our proposed alternative interface system more objectively, we have developed Fitts' law [12] based operability test GUI (Fig. 6) which was extended to two-dimensional model in contrast with the traditional model taking one-dimensional model. Fitts' law is used to model the action of pointing, either by physically touching an object with a hand or finger, or virtually, by pointing to an object on a computer screen using a pointing device. It is, therefore, useful to be aware of the operability of a new computer pointing device and to compare it with other computer pointing device. According to Fitts' law, the movement time (MT) of the cursor to a target and the task difficulty (ID: index of difficulty) have the following linear relationship,

$$MT = \alpha + \beta ID, \tag{4}$$

where α represents the start/stop time of the device (intercept) and β stands for the inherent speed of the device (slope). The reciprocal number of β is called the index of performance (IP) in bits per second and IP represents how quickly the pointing and clicking can be performed with the computer pointing device. The equation shows that an interface with a high IP is better than that with a lower IP, because a high IP indicates that the device performance is less affected by a high ID.

The ID depends on the (W), which is equal to diameter of the target circle in our model, and the distance (D) between the cursor and the target. The ID is defined as follows,

$$ID = \log_2 \left(1 + \frac{D}{W} \right). \tag{5}$$

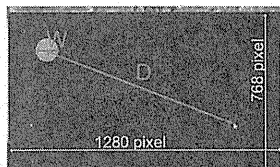


Fig. 6. Fitts' law based test GUI

Thus, it is obvious that the task becomes more difficult as D increases or W decreases. The operability parameter IP and also the parameter α are determined experimentally in following section.

B. Experimental condition and subject information

The two-dimensional Fitts' law based test GUI is shown in Fig. 6. Eighty number of cyan colored circle targets, the size and location of which are random ($30 < W < 300$ pixel), appear in order in the black screen after the former target is clicked correctly. The MT is measured as time interval between the former target and the next target.

The test was conducted in two sessions. The first session

used a mouse interface and second used our proposed interface system. Four subjects (S1-S4) with intact limbs (four males, average 25 years old) volunteered and sat comfortably in front of the computer screen showing the test bed GUI and were instructed to point to and click a circle target by moving the cursor. Since the S1 developed this system, he was comparatively habituated to use it. Others use this proposed interface system for the first time.

The correspondence between the channels and the mouse actions are described in Table 2. One trial requests the subject to click the target eighty times. The subject did 15 trials with our proposed interface and did a trial with mouse interface. Every trial was done in one day. Then the system evaluated by IP.

C. Experimental results

Some of experimental results are shown in Fig. 6. Each graph represents the relationship between the MT and the ID of the each trial. From these graphs, the IPs are calculated. Figure 7 shows the transition of the IP during the experiment. It is obvious that the subject had progressed while repeating the practice and that the proposed system is easy to learn. The maximum scores of the subject 1, 2, 3 and 4 are IP=1.873, 1.3, and 1.2, 0.8 respectively.

Table 3 shows a comparison of our proposed interface systems with other alternative interface systems by the IP. Our proposed system outperforms the system proposed in [2] using BMI, in [13] using forearm myoelectricity.

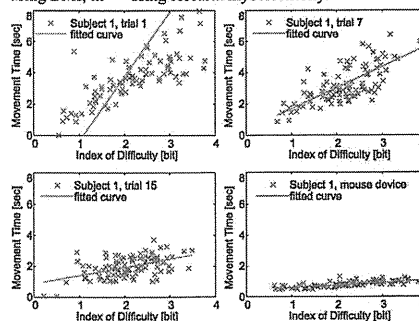


Fig. 6. Some of Experimental results plotted on ID versus MT graph

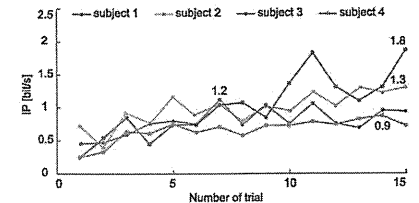


Fig. 7. Transition of the IP

TABLE 3
COMPARISON WITH RELATED STUDIES IN IP

	Brain finger [2]	Forearm Myoelectricity [13]	Proposed method	Mouse our data	Mouse [13]
IP bits/s	0.386	1.34	1.87	6.09	9.60

5. CONCLUSION

This paper proposed an alternative interface system by extracting a human intention from his/her surface electromyogram registered on the skin surface. To realize an alternative interface system, we developed discriminant criteria to detect operational intention from various patterns of myoelectric signals. The criteria are for detecting special patterns of myoelectric signals as operational intentions. The special patterns of the signals are consisted of the simultaneous contraction of agonist and antagonist muscles of elbow joints, the simultaneous contraction of right and left of upside trapezius, and the simultaneous contraction of latissimus dorsi.

The discriminant criteria were evaluated and were validated experimentally. The results show that the system can be utilized by a user while doing other works except for lifting something with both hands. Next, the special patterns of myoelectric signals are associated with the movements of cursor pointer (right, left, up, and down) to organize an alternative interface system. The operability of the proposed interface system was evaluated with Fitts' law based operability test bed by four subjects. The results, the best score of which is IP=1.83, show that the proposed system overcomes other related studies in IP comparison.

This alternative interface system enables both arms amputee to utilize a computer by controlling mouse cursor more quickly and smoothly so that they get back into society. Additionally, the concept, which is taking advantage of residual muscles, can be applied for other types of physically challenged person, such as spinal cord injury, muscle dystrophy and paralyzed patient.

One of the future works is to develop an auto-calibration algorithm for normalization of myoelectric signal and for deciding a threshold k so that a user does not have to do the MVC based normalization process manually. If it realized, the usability of proposed system becomes dramatically better. Another is to develop a whole system including electrodes, amplify, calculator, and connection part for each individual case of a physically challenged person.

REFERENCES

[1] Sanchez, JC and Principe, JC and Nishida, T. and Bashirullah, R. and Harris, JG and Fortes, JAB, "Technology and signal processing for brain-machine interfaces," IEEE Signal Processing Magazine, vol. 25, no. 1, pp.29-40, 2008

[2] A. Pino, E. Kalogeros, E. Salemis, and G. Kouroupetroglou, "Brain Computer interface cursor measures for motion-impaired and able-bodied users," *Int. Conf. Human-Comput. Interact.*, 4, pp.

1462-1466, 2003.

[3] Cipriani, C. and Zaccone, F. and Micera, S. and Carrozza, M.C., "On the shared control of an EMG-controlled prosthetic hand: analysis of user-prosthesis interaction," IEEE Trans. on Robotics, vol. 24, NO. 1, pp. 170-184, 2008.

[4] Engeberg, E.D. and Meek, S.G., "Backstepping and Sliding Mode Control Hybridized for a Prosthetic Hand," IEEE Trans. on Neural Systems and Rehabilitation Engineering, vol.17, NO. 1, pp.70-79, 2009

[5] Kawamoto, H. and Lee, S. and Kanbe, S. and Sankai, Y., "Power assist method for HAL-3 using EMG-based feedback controller," IEEE Int. Conf. on Systems, Man and Cybernetics, vol. 2, pp. 1648-1653, 2003.

[6] Fleischer, C. and Hommel, G., "A Human-Exoskeleton Interface Utilizing Electromyography," IEEE Trans. on Robotics, vol. 24, NO. 4, pp. 872-882, Aug. 2008.

[7] Englehart, K. and Hudgin, B. and Parker, P.A., "A wavelet-based continuous classification scheme for multifunction myoelectric control," Biomedical Engineering, IEEE Transactions on, vol. 48, No. 3, pp. 302-311, 2001.

[8] Englehart, K. and Hudgins, B., "A robust, real-time control scheme for multifunction myoelectric control," Biomedical Engineering, IEEE Transactions on, vol. 50, no. 7, pp. 848-854, 2003.

[9] Asghari Oskoei, M. and Hu, H., "Myoelectric control systems -A survey," Biomedical Signal Processing and Control, vol. 2, no. 4, pp. 275-294, 2007.

[10] Kato, R. and Yokoi, H. and Hernandez Arieta, A. and Yu, W. and Arai, T., "Mutual adaptation among man and machine by using f-MRI analysis," Robotics and Autonomous Systems, 57, 2, pp.161-166, 2009.

[11] Takahashi, Junji, Hasegawa, Yasuhisa, and Sankai, Yoshiyuki, "Alternative Interface System by Using Surface Myoelectricity from Unusual Muscles Contraction," Proc. of IEEE International Conference on Robotics and Automation, pp.4513-4518, 2012

[12] Fitts, P.M. "The information capacity of the human motor system in controlling the amplitude of movement," Journal of Experimental Psychology, Vol. 47, No. 6, pp. 381-391, 1954

[13] Choi, C. and Micera, S. and Carpaneto, J. and Kim, J., "Development and quantitative performance evaluation of a noninvasive EMG computer interface," IEEE Trans. on Biomedical Eng., vol. 56, NO. 1, Jan. 2009.



Junji Takahashi graduated from Nagoya University and received the Ph.D. degree in Engineering in 2010. He had been a Research Fellow on GCOE (Cybernetics) at the Graduate School of Systems and Information Engineering in University of Tsukuba for April 2010 to March 2012. Currently, he is a postdoctoral Research Fellow of the Department of Micro-Nano Systems Engineering in Nagoya University. He will be an Assistant

Professor of Aoyama Gakuin University, from April 2013. His research interests are Mechatronics, Distributed Autonomous Robotic Systems, Human Robot Interaction, and Bio-signal Processing. He is a member of IEEE, RSJ, and SICE. He received a Best Paper Award at the 9th International Symposium on Distributed Autonomous Robotic Systems (DARS2008), a prize of encouragement from the Chubu Branch of The Society of Instrument and Control Engineers (SICE), 2012.



Yoshiyuki Sankai received his Ph.D. degree in engineering from University of Tsukuba, Japan in 1987. He was formerly Assistant Professor, Associate Professor and Professor in the Institute of Systems and Engineering, University of Tsukuba, and Visiting Professor at Baylor College of Medicine, Houston, Texas, in the United States of America. He was the leader of the Global COE (Centre of Excellence) program for Cybernetics at University of Tsukuba. He is currently a Professor of the Graduate School in Systems and Information Engineering, the Director of the Center for Cybernetics Research, University of Tsukuba, the President/CEO of CYBERDYNE Inc. and the Leader of "FIRST" (Funding Program for World Leading Innovative R&D on Science and Technology) on Cybernetics, funded by the Cabinet office of Japan. He is an Executive Board Member of the Japan Society of Embolus Detection and Treatment, the Fellow of the Robotics Society of Japan (RSJ), Advisory Committee of RSJ International Journal, and also an executive editor of Vascular Lab. He has won the World Technology Award (2005), the METI (Minister of Economy, Trade and Industry of Japan) Minister Award (2007), the 21st century Invention Award from Japan Institute of Invention and Innovation (2009) and other awards



Noel Segura Meraz received his bachelor degree in Mechatronics Engineering from the Instituto Tecnológico de Estudios Superiores de Monterrey campus Puebla, Mexico in 2008. He was Laboratory professor at ITESM campus Puebla, Mexico from January 2009 to January 2010. From April 2010 to March 2011 he was research student at the Graduate School of Systems and Information Engineering in the University of Tsukuba. Since April 2012 he belongs to the master program on Intelligent Interaction Technologies on the University of Tsukuba



Yasuhisa Hasegawa received his Ph.D degree in engineering from Nagoya University, Japan in 2001. From 1996 to 1998, he worked for Mitsubishi Heavy Industries Ltd., Japan. He was formerly a Research Associate at Nagoya University, an Assistant Professor at Gifu University, and an Assistant Professor at University of Tsukuba. He is currently an Associate Professor of the Graduate School in Systems and Information Engineering, and of Center for Cybernetics Research, University of Tsukuba. He is also a Deputy Chief Editor of Journal of Robotics and Mechatronics (JRM) and a member of board of directors of the Robotics Society of Japan (RSJ). He is mainly engaging in the research fields of human intention-based physical assistive robot, dexterous manipulation and dynamic motion control. He received a Best Paper Award at the 2003 IEEE/RSJ International Conference on Intelligent Robots and Systems (IROS2003) and at the 2004 International Symposium on Micro-Nano Mechatronics and Human Science (MHS2004).

Available online at:
<http://tsest.org/index.php/TCMS/article/view/106>

Download full text article at:
<http://tsest.org/index.php/TCMS/article/download/106/65>

Cite this work as:

Junji Takahashi, Noel Segura Meraz, Yasuhisa Hasegawa, and Yoshiyuki Sankai, "The Discriminant Criteria Detecting Operational Intention from Myoelectricity for Alternative Interface System," *TSEST Transaction on Control and Mechanical Systems*, Vol. 2, No. 1, Pp. 13-19, Jan., 2013.



ORIGINAL ARTICLE

Feasibility of Rehabilitation Training With a Newly Developed Wearable Robot for Patients With Limited Mobility

Shigeki Kubota, MS, OT,^a Yoshio Nakata, PhD,^{b,c} Kiyoshi Eguchi, MD, PhD,^b Hiroaki Kawamoto, PhD,^d Kiyotaka Kamibayashi, PhD,^d Masataka Sakane, MD, PhD,^{b,c} Yoshiyuki Sankai, PhD,^d Naoyuki Ochiai, MD, PhD^{b,c}

From the ^aGraduate School of Comprehensive Human Sciences, ^bFaculty of Medicine, ^cTsukuba Critical Path Research and Education Integrated Leading Center (CREIL), and ^dFaculty of Systems and Information Engineering, University of Tsukuba, Ibaraki, Japan.

Abstract

Objective: To investigate the feasibility of rehabilitation training with a new wearable robot.

Design: Before-after clinical intervention.

Setting: University hospital and private rehabilitation facilities.

Participants: A convenience sample of patients (N=38) with limited mobility. The underlying diseases were stroke (n=12), spinal cord injuries (n=8), musculoskeletal diseases (n=4), and other diseases (n=14).

Interventions: The patients received 90-minute training with a wearable robot twice per week for 8 weeks (16 sessions).

Main Outcome Measures: Functional ambulation was assessed with the 10-m walk test (10MWT) and the Timed Up & Go (TUG) test, and balance ability was assessed with the Berg Balance Scale (BBS). Both assessments were performed at baseline and after rehabilitation.

Results: Thirty-two patients completed 16 sessions of training with the wearable robot. The results of the 10MWT included significant improvements in gait speed, number of steps, and cadence. Although improvements were observed, as measured with the TUG test and BBS, the results were not statistically significant. No serious adverse events were observed during the training.

Conclusions: Eight weeks of rehabilitative training with the wearable robot (16 sessions of 90min) could be performed safely and effectively, even many years after the subjects received their diagnosis.

Archives of Physical Medicine and Rehabilitation 2013; 94(12): 2120-2125

© 2013 by the American Congress of Rehabilitation Medicine

Rehabilitation robotics emerged in the 1980s with the aim of using robotic technology to assist people with movement dysfunction.¹ Robotic devices have recently been developed for use in clinical settings. Tefertiller et al² reviewed 30 articles (14 randomized

controlled trials, 16 nonrandomized controlled trials) that examined the effects of locomotor training with robotic assistance in patients after stroke, spinal cord injury (SCI), multiple sclerosis, traumatic brain injury, and Parkinson's disease. The review supports the conclusion that locomotor training with robotic assistance is beneficial for improving walking function in individuals after stroke and SCI.² The development of main gait training machines followed. These machines either involve an exoskeleton robotic device (eg, Lokomat, LOPES exoskeleton robot)^{3,4} or a robotic device with foot-driven plates (eg, Gait Trainer GT I, Haptic Walker).^{5,6} The exoskeleton robotic device is equipped with programmable drives or passive elements that flex the knees and hips during the swing phase, whereas with the other type of robotic device, the feet are placed on footplates, whose trajectories simulate the stance and swing phases. Other than robotic gait training and conventional therapy, another treatment

approach involves treadmill training with partial body weight support.⁷ However, this approach requires considerable involvement of a physical therapist, and generally, 3 therapists are required to induce movement of the paretic leg during the swing phase and to shift the patient's weight onto the stance limb.

The potentially positive common benefits of robotic gait training are that it involves repeatedly undergoing sufficient and accurate training for a prolonged period. Lokomat is the first robotic-driven gait orthosis with electromechanical drives to assist the walking movements of gait-impaired patients on a treadmill by supporting the body weight.^{8,9} Husemann et al¹⁰ compared a Lokomat group that received 30 minutes of robotic training with a control group that received 30 minutes of conventional physiotherapy. After 4 weeks of therapy, although there was no significant difference in walking ability between the groups, the walking ability in both groups as expressed by functional ambulation classification was significantly improved. The researchers reported that the Lokomat group demonstrated an advantage for robotic training over conventional physiotherapy in the improvement of gait abnormality and body tissue composition.¹⁰ However, in a recent randomized controlled study¹¹ that compared robot-assisted locomotor training with therapist-assisted locomotor training in chronic stroke patients, the results indicated that greater improvements in speed and single limb stance time on the impaired leg were observed in subjects who received therapist-assisted locomotor training. Thus, the usefulness of robot-assisted rehabilitation is controversial.

The robot suit hybrid assistive limb (HAL)^{12-15a} is a new wearable robot that has a hybrid control system composed of 2 subsystems: cybernetic voluntary control (CVC) and cybernetic autonomous control (CAC) (fig 1). The HAL suit has power units and force-pressure sensors in the shoes. The power units consist of angular sensors and actuators on bilateral hip and knee joints. Muscle action potentials are detected through the electrodes on the anterior and posterior surface of the wearer's thigh. These various biologic signals are processed by a computer. The HAL suit can support the wearer's motion by adjusting the level and timing of the assistive torque provided to each joint according to the surface muscle action potential as well as the pressure sensors. The HAL suit can enhance the wearer's motion through the wearer's muscle action potential; thus, the HAL suit can appear as an actual motion. Therefore, if the wearer's muscle action potential varies, the wearer's motion varies, too. The HAL training, using muscle activity, has the potential to intensify the feedback by inducing an appropriate motion more strongly than standard robot training. Thus, after HAL training, patients with limited mobility will improve their walking abilities (gait speed, number of steps, cadence, or ability to transfer).

Few studies have been conducted to clarify the feasibility of rehabilitation with HAL. Only 1 preliminary study¹⁶ has reported on the short-term effects of HAL on the walking pattern of stroke

patients. The purpose of the present study was to investigate the feasibility of 16-session (8-wk) HAL rehabilitation training for patients with limited mobility.

Methods

Study design

A quasiexperimental study was used, with measurements before and after the clinical intervention. The target population included patients with limitations in their walking (no matter the diagnosis, the time since the diagnosis, and the patient's age at diagnosis). The protocol of this study was approved by the Institutional Review Board of the University of Tsukuba Hospital and was registered with the UMIN Clinical Trials Registry. The clinical intervention was conducted at the University of Tsukuba Hospital and Cyberdyne, Inc, in Japan between January 2010 and March 2012. The patients included in this study were volunteers recruited through local newspaper advertisements or outpatients at the University of Tsukuba Hospital. They were informed about the aim and design of this study, and they subsequently provided written, informed consent. Informed consent was also obtained from the patient's guardian if the patient was younger than 20 years.

The inclusion criteria were (1) musculoskeletal ambulation disability symptom complex (MADS) or the underlying disorders of MADS, which is a condition newly defined in 2006 by Japanese medical societies¹⁷; (2) requiring physical assistance or assistive devices in at least 1 of the following daily activities: standing up, sitting down, and walking; (3) ability to understand an explanation of the study and to express consent or refusal; (4) body size that can fit in the robotic suit HAL (height range, 145–180cm; maximal body weight, 80kg); and (5) ability to undergo usual physical and occupational therapies. The exclusion criteria were the following: (1) inadequately controlled cardiovascular disorders; (2) inadequately controlled respiratory disorders; (3) intellectual impairments that limit the ability to understand instructions; (4) moderate to severe articular disorders, including contracture in the lower extremities; (5) moderate to severe involuntary movements, ataxia, or impairments of postural reflex in the trunk or the lower extremities; and (6) severe spasticity in the lower extremities.

Participants

Thirty-eight patients (25 men, 13 women) were enrolled in this study (24 outpatients, 14 volunteers through advertisements). The mean age ± SD of the 38 patients was 53.2±17.8 years (range, 18–81y). Table 1 summarizes their clinical characteristics. Their underlying diseases were stroke (10 men, 2 women), SCI (6 men, 2 women), musculoskeletal diseases (2 men, 2 women), and other diseases (Parkinson's disease, gonadotropin-dependent myopathy, limb-girdle muscular dystrophy, inclusion body myositis, traumatic brain injury, disuse syndrome secondary to malignant lymphoma, cerebral palsy, sequelae of poliomyelitis, and hypoxic-ischemic encephalopathy; 7 men, 7 women). Twenty patients were able to ambulate independently without any help (n=9) or with several assistive devices (T-cane, bilateral crutches, or lateral crutch) (n=11). Eleven patients were able to ambulate with several assistive devices and under supervision. Three patients required human assistance to ambulate at least 10m (cases 33, 34, 38), and the remaining 4 patients were unable to ambulate even

List of abbreviations:

BBS	Berg Balance Scale
CAC	cybernetic autonomous control
CVC	cybernetic voluntary control
HAL	hybrid assistive limb
MADS	musculoskeletal ambulation disability symptom complex
SCI	spinal cord injury
10MWT	10-m walk test
TUG	Timed Up & Go

Supported by the "Center for Cybernetic Research—World Leading Human-Assistive Technology Supporting a Long-Lived and Healthy Society," granted through "Funding Program for World-Leading Innovative R&D on Science and Technology (FIRST Program)," initiated by the Council for Science and Technology Policy.

A commercial party having a direct financial interest in the results of the research supporting this article has conferred or will confer a financial benefit on 1 or more of the authors. Yoshiyuki Sankai is CEO of Cyberdyne Inc, Ibaraki, Japan. Hiroaki Kawamoto is a stockholder of the company. Cyberdyne is the manufacturer of the robot suit HAL. This study was proposed by the authors. Cyberdyne was not directly involved in the study design, collection, analysis, or interpretation of data; writing the report; or the decision to submit the paper for publication.

No commercial party having a direct financial interest in the results of the research supporting this article has or will confer a benefit on the authors or on any organization with which the authors are associated (Kubota, Nakata, Eguchi, Kamibayashi, Sakane, Ochiai).

Clinical Trial Registry Number: UMIN00002969.

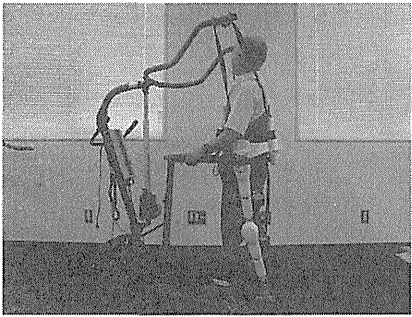


Fig 1 The robot suit HAL.

with assistive devices and human assistance (cases 8, 15, 17, 27). All the patients with stroke and SCI were in chronic stages.

Training program

HAL training was administered twice per week for 8 weeks (16 sessions). The 90-minute training sessions consisted of single-leg motion, a standing and sitting exercise, and walking on the ground with HAL. For safety reasons, a walking device (All-in-One Walking Trainer[®]) with a harness was used. Treadmill training with mild body-weight support (Unweighing System[®]) was also used for some patients. The HAL suit has a hybrid control system comprising the CVC and CAC. The CVC mode of the HAL suit can support the patient's voluntary motion according to the voluntary muscle activity and the assistive torque provided to each joint. The CAC mode provides physical support autonomously, based on output from force-pressure sensors in the shoes. This study mainly used the CVC mode, which allows the operator to adjust the degree of physical support to the patient's comfort and gradually reduce support as training progresses.

Outcome measures

The feasibility of rehabilitation with HAL was assessed by the number of completers and the amount of time or the number of therapists needed to implement training. Patients were asked to report adverse events during the training period.

The primary outcomes were functional ambulation and balance ability. Functional ambulation was assessed with a 10-m walk test (10MWT) and a Timed Up & Go (TUG) test. In the 10MWT, patients were instructed to walk without wearing HAL on a flat surface at their self-selected, comfortable pace. Patients began to walk before they reached the starting line of the 10-m distance so that they could accelerate and attain a stable speed before the test. To calculate gait speed (m/s) as a primary outcome, the 10-m walking time was measured using a handheld stopwatch. In addition, the number of steps between the start and finish line was counted, and patient cadence was calculated from the walking time and number of steps. Patients were allowed to use their assistive device or lower limb orthosis, or both, as necessary. Each patient used the same assistive device or orthosis, or both, during

the pre- and postintervention measurements. Therapists closely attended the patients during the 10MWT but did not provide physical assistance. For each measurement, the 10MWT was performed twice. The faster time of 2 trials was selected for analysis. In the TUG test, the following actions were timed: standing up from a standard-height chair, walking 3m, returning to the chair, and sitting down without HAL. Two trials (each turning clockwise and counterclockwise) were carried out for each measurement. Balance ability was assessed with the Berg Balance Scale (BBS), consisting of 14 tasks, as detailed by Berg et al.¹⁸ Each task was scored on a scale ranging from 0 to 4 points (0 indicates inability to complete), and the total score was used as the index of balance ability. All primary outcomes were assessed at baseline and after completion of the 16 training sessions.

Statistical analysis

All parametric data are expressed as means with SDs. Paired *t* tests were used to evaluate differences between the baseline measurements and outcomes after the 16 sessions. Unpaired *t* tests were used to evaluate the differences in characteristics of those who completed 16 sessions and those who did not. An effect-size calculation (Cohen *d*) was used to assess the effect of the training. Pearson correlation coefficients were used to assess the relationship among outcome measures. Data were analyzed using IBM SPSS Statistics 18 software,⁴ with the alpha level set at 5%.

Results

A typical 90-minute HAL training session proceeded as follows: assessment of blood pressure, resting heart rate, and walking pattern (10min); preparation of electrodes and putting on the HAL suit (5min); computer setup (5min); HAL training (60min, including resting time during computer operation); taking off the HAL suit and the electrodes (5min); and reassessment of walking pattern (5min). The net walking time was approximately 20 minutes. Typically, 2 therapists implemented the training: one supported the patient and the other operated the computer. All therapists and related staff had participated in a 3-hour training workshop conducted by the manufacturer to learn how to operate the HAL system.

Of the 38 patients (25 men, 13 women), 32 (21 men, 11 women) completed all 16 training sessions. The mean age ± SD of the 32 patients was 53.2±17.3 years (range, 18–81y). There was no statistically significant difference in age between those who completed training and those who did not (54.0±19.8y). It took 10.0±3.1 weeks (range, 8–21wk) to complete 16 sessions. Of the 6 patients who did not complete the 16 sessions, 2 (cases 15, 21) dropped out for medical reasons, and 4 (cases 1, 2, 29, 35) dropped out for personal reasons (difficulty visiting the hospital). One medical reason for dropout was low back pain that developed during the first training session (case 21); the patient withdrew consent at the third session. The other medical reason for dropout was a relapse (after the second session) of neuropathic pain caused by SCI (case 15); the patient withdrew consent at the fifth session. There were no serious training-related adverse events. One stroke patient (case 7) had knee pain (patellar tendinitis) at home after the 15th session but was able to complete the 16th session after 1 month of rest. Another patient with inclusion body myositis (case 31) developed knee

Table 1 Clinical characteristics of patients

Case No.	Age (y)	Sex	Diagnosis	Paralysis Type	Duration Since Disease	Ambulation	Assistive Device	Orthosis	Training	Duration of Training (wk)	Adverse Events
1	69	M	Stroke (cerebral infarct)	Paraplegia	15y	Independently	T-cane	AFO	Dropout (personal reason)	ND	Nothing
2	61	M	Stroke (cerebral hemorrhage)	Paraplegia	14y6mo	Independently	T-cane	AFO	Dropout (personal reason)	ND	Nothing
3	65	M	Stroke (cerebral hemorrhage)	Hemiplegia	2y2mo	Supervision	Quad-cane	AFO	Complete (reason)	8	Nothing
4	37	F	Stroke (cerebral hemorrhage)	Quadriplegia	16y	Independently	NA	AFO	Complete	8	Nothing
5	72	M	Stroke (cerebral infarct)	Hemiplegia	2y9mo	Supervision	T-cane	AFO	Complete	8	Nothing
6	54	M	Stroke (cerebral hemorrhage)	Hemiplegia	1y1mo	Supervision	T-cane	NA	Complete	8	Nothing
7	63	F	Stroke (cerebral hemorrhage)	Hemiplegia	1y6mo	Independently	T-cane	AFO	Complete	15	Knee pain (patellar tendinitis)
8	52	M	Stroke (cerebral hemorrhage)	Ataxia	2y2mo	NA	NA	NA	Complete	12	Nothing
9	74	M	Stroke (cerebral infarct)	Hemiplegia	3y4mo	Independently	T-cane	AFO	Complete	9	Nothing
10	53	M	Stroke (subarachnoid hemorrhage, cerebral infarct)	Hemiplegia	ND	Supervision	Pick-up walker	KARO	Complete	9	Nothing
11	18	M	Stroke (meningoencephalitis)	Hemiplegia	11y	Independently	NA	AFO	Complete	21	Nothing
12	64	M	Stroke (cerebral hemorrhage)	Hemiplegia	1y	Supervision	T-cane	AFO	Complete	8	Nothing
13	58	F	Stroke (cerebral hemorrhage)	Quadriplegia	3y3mo	Supervision	Lateral crutch	KARO	Complete	8	Nothing
14	69	M	SCI (incomplete)	Quadriplegia	1y3mo	Supervision	Pick-up walker	AFO	Complete	8	Nothing
15	43	M	SCI (incomplete)	Paraplegia	3y3mo	NA	NA	KARO	Dropout (medical reason)	ND	Neuropathic pain after SCI
16	59	M	SCI (spina bifida)	Paraplegia	6y4mo	Supervision	T-cane	NA	Complete	8	Nothing
17	31	M	SCI (complete)	Paraplegia	3y	NA	NA	NA	Complete	10	Nothing
18	64	F	SCI (incomplete)	Quadriplegia	2y	Independently	T-cane	AFO	Complete	9	Nothing
19	54	M	SCI (central cervical cord injury)	Quadriplegia	5y	Supervision	T-cane	NA	Complete	12	Nothing
20	47	M	SCI (spinal dural arteriovenous fistula)	Paraplegia	1y1mo	Independently	Bilateral crutch	AFO	Complete	8	Nothing
21	74	F	Musculoskeletal disease (cervical spondylosis myelopathy)	Quadriplegia	ND	Independently	Bilateral crutch	NA	Dropout (medical reason)	ND	Low back pain
22	81	F	Musculoskeletal disease (OA, knee)	NA	ND	Independently	NA	NA	Complete (reason)	10	Nothing
23	44	M	Musculoskeletal disease (OA, knee)	NA	ND	Independently	NA	NA	Complete	11	Nothing
24	74	M	Musculoskeletal disease (OA, knee)	NA	ND	Independently	NA	NA	Complete	10	Nothing
25	62	M	Parkinson's disease	NA	8y	Independently	NA	NA	Complete	11	Nothing

(continued on next page)

Table 2 Functional ambulation and balance ability at baseline and after 16-session HAL training

Outcome Measurements	Baseline	After Training	Difference	P	n
10MWT					
Speed (m/s)	0.52±0.40	0.61±0.43	0.09 (0.05 to 0.14)	<.001	27
No. of steps	34.0±20.4	31.0±18.8	-3.0 (-4.9 to -1.0)	<.001	27
Cadence (steps/min)	74.3±34.1	81.1±32.9	6.8 (4.0 to 9.6)	<.001	27
TUG (s)	43.7±45.0	37.3±34.1	-6.4 (-13.0 to 0.2)	.057	26
BBS	33.6±16.9	35.5±16.3	1.9 (-0.1 to 3.9)	.059	32

NOTE. Values are mean ± SD, mean (95% confidence interval), or as otherwise indicated.

pain at home after an early session but was able to complete 16 sessions.

Outcome measures

Functional ambulation was not assessed for 5 patients at baseline because 3 were unable to ambulate with any assistance (cases 8, 17, 27), and the other 2 patients needed considerable human assistance to ambulate (cases 34, 38). The other 27 patients had significant improvements ($P<.05$) in gait speed, number of steps, and cadence after the 16-session HAL training (10MWT, table 2). Improvements in gait speed, number of steps, and cadence are defined as an increase, a decrease, and an increase in the respective parameters. The mean ± SD improvements and effect sizes (Cohen d) in gait speed, number of steps, and cadence were .09±.11 m/s ($d=.82$), 3.0±4.9 steps ($d=.61$), and 6.8±7.1 steps/min ($d=.96$), respectively. Improvements in gait speed, steps, and cadence were observed in 25, 18, and 25 patients, respectively (figs 2–4). Worsened gait speed and cadence were observed in 2 patients (cases 28, 30). In regards to the number of steps, we observed no change in 8 patients (cases 3, 5, 16, 25, 28, 30, 33, 37) and increased steps in 1 (case 20). Correlation coefficients for gait speed with number of steps and with cadence were $r=.30$ (not significant) and $r=.73$ ($P<.01$), respectively. The effect sizes for gait speed in patients with stroke ($n=9$), SCI ($n=6$), musculoskeletal disease ($n=3$), and patients with other diseases ($n=9$) were 1.41, .78, 2.43, and .63, respectively. The results of the TUG test ($n=26$; case 10 was unable to perform the

test) and the BBS ($n=32$) indicated improvement after the 16 training sessions, but these improvements were not statistically significant. The mean ± SD decrease (Cohen d) in the TUG test was 6.4±16.4 seconds ($d=.39$). Twenty-one of 26 patients were faster after training, and 5 patients were slower (cases 5, 13, 30, 31, 36) (fig 5). The mean ± SD increase (Cohen d) in BBS was 1.9±5.5 ($d=.35$). Nineteen of 32 patients had higher scores compared with baseline; no change was observed in 6 (cases 12, 17, 23, 27, 36, 37), and 7 had lower scores (cases 11, 16, 26, 30, 31, 32, 34) (fig 6).

Discussion

We investigated the feasibility of rehabilitation using a robot suit HAL. We demonstrated that HAL rehabilitation could be implemented safely and effectively. Although a few patients developed lumbar or knee pain during the training, no serious training-related adverse events occurred. Significant improvements in gait speed, number of steps, and cadence were observed, as assessed by the 10MWT. Improved TUG test and BBS results were also observed, but because of the small sample size of this pilot study, these improvements were not statistically significant. Overall, our results suggest that HAL rehabilitation has the potential to improve ambulation in patients with limited mobility.

Two patients (cases 15, 21) dropped out for medical reasons. One developed lumbar pain (case 21), and 1 had a relapse of neuropathic pain caused by SCI (case 15). Although it is unclear

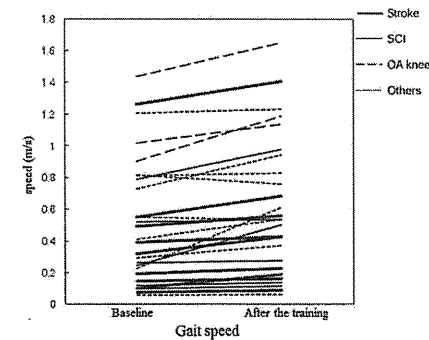


Fig 2 Change in 10MWT gait speed for 27 patients after HAL training. Abbreviation: OA, osteoarthritis.

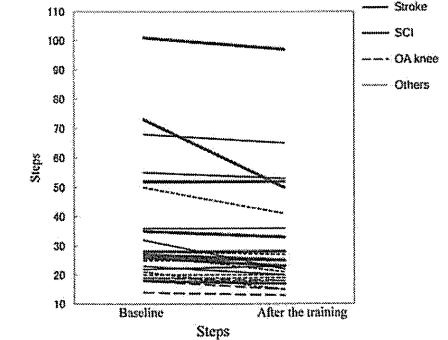


Fig 3 Change in number of steps during 10MWT for 27 patients after HAL training. Abbreviation: OA, osteoarthritis.

Table 1 (continued)

Case No.	Age (y)	Sex	Diagnosis	Paralysis Type	Duration Since Disease	Ambulation	Assistive Device	Orthosis	Training (reason)	Duration of Training (wk)	Adverse Events
26	72	F	Parkinson's disease	NA	7y6mo	Independently	Nothing	NA	Complete	9	Nothing
27	36	M	Gonadotrophin-dependent myopathy	Paraplegia	1y	NA	Nothing	NA	Complete	8	Nothing
28	52	F	Limb-girdle muscular dystrophy	Quadruplegia	24y	Supervision	T-cane	NA	Complete	9	Nothing
29	57	F	Muscular dystrophy	NA	44y	Independently	NA	NA	Dropout (personal reason)	ND	Nothing
30	67	M	Limb-girdle muscular dystrophy	NA	26y	Independently	T-cane	NA	Complete	8	Nothing
31	73	M	Inclusion body myositis	Quadruplegia	10y	Independently	T-cane	NA	Complete	10	Knee pain
32	24	M	Traumatic brain injury	Quadruplegia	17y1mo	Supervision	Walker	NA	Complete	8	Nothing
33	19	F	Traumatic brain injury	Quadruplegia	6y2mo	Assistance	Pick-up walker	KARO	Complete	8	Nothing
34	29	F	Traumatic brain injury	Quadruplegia	10y7mo	Assistance	Pick-up walker	KARO	Complete	9	Nothing
35	20	M	Disuse syndrome, secondary to malignant lymphoma	NA	3y9mo	Independently	T-cane	NA	Dropout (personal reason)	ND	Nothing
36	31	F	Cerebral palsy	Quadruplegia	30y10mo	Independently	Lateral crutch	NA	Complete	10	Nothing
37	55	M	Sequelae of poliomyelitis	Paraplegia	54y	Independently	Lateral crutch	NA	Complete	19	Nothing
38	48	F	Hypoxic-ischemic encephalopathy	Quadruplegia	2y	Assistance	Nothing	NA	Complete	12	Nothing

Abbreviations: RO, ankle-foot orthosis; F, female; KARO, knee-ankle-foot orthosis; M, male; NA, not applicable; ND, no data; OA, osteoarthritis.

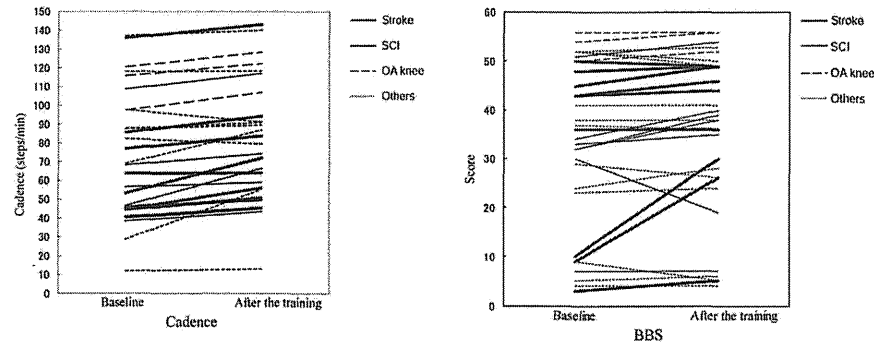


Fig 4 Change in 10MWT cadence for 27 patients after HAL training. Abbreviation: OA, osteoarthritis.

whether there was a causal relationship between HAL training and the pain that developed, the lumbar pain in case 21 had been persistent before the HAL training and even after the training ended, and the neuropathic pain in case 15 followed a previous pattern of symptom flares associated with seasonal change. Therefore, it is likely that HAL training did not directly cause the pain that developed in these 2 cases. Two other patients complained of knee pain during the training period, but this pain was not severe, and the patients were able to complete the training. Although, once again, direct causality is unclear, safe implementation of HAL rehabilitation requires adequate caution on the part of therapists and self-awareness on the part of patients who have lumbar and knee pain. Regarding feasibility, approximately 10 minutes was required for 2 to 3 therapists to put electrodes and the HAL suit on or take them off the patient. This procedure is a slight inconvenience to address but not a major obstacle to HAL rehabilitation.

Significant improvements in functional ambulation were observed, and the effect sizes (Cohen *d*) for gait speed, number of steps, and cadence were .82, .61, and .96, respectively. The correlation coefficient for gait speed with cadence was higher than

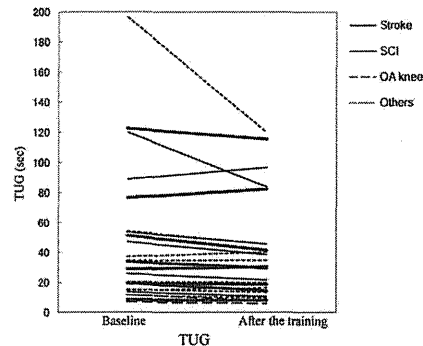


Fig 5 Change in TUG test results for 26 patients after HAL training. Abbreviation: OA, osteoarthritis.

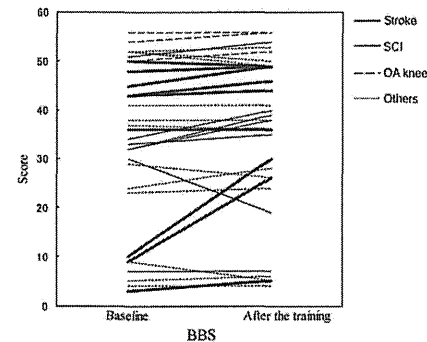


Fig 6 Change in BBS score for 32 patients after HAL training. Abbreviation: OA, osteoarthritis.

that of gait speed with steps ($r=.73$ vs $r=.30$). Therefore, the improvement in gait speed with HAL training was mainly brought about by improvement in cadence. That is, HAL training improved stride frequency more than stride length. This finding is in agreement with that of a previous robotic training study.¹⁹ The effect sizes for the TUG test and BBS were smaller than the effect sizes for the 10MWT. This result seems to occur because the TUG test and BBS involve complicated motions such as moving from sitting to standing, walking and returning, reaching forward, and alternating feet on each step. The effect sizes for gait speed in 9 patients with stroke and in 6 patients with SCI were large (1.41 and .78, respectively). Therefore, training effectiveness in patients with stroke and those with SCI can be expected. The effect size in 3 patients with musculoskeletal diseases was also large (2.43), but the number of patients was small. Therefore, further studies are needed. In this study, we recruited patients with a wide range of stroke and SCI severities. Future studies should examine the influence of the severity of stroke and SCI on the effectiveness of HAL rehabilitation.

Many recent studies have reported the efficacy of robot-assisted rehabilitation. It is very difficult to directly compare these studies and our study, because of differences in diseases, severity and duration of the disorder, robotic features, methods of intervention, and outcome measures.²⁰ Wirz et al²¹ reported that after locomotor training with Lokomat, the 10MWT gait speed of 20 patients with chronic incomplete SCI increased by $.11 \pm .10$ m/s ($d=1.10$). The number of patients with SCI in our study was limited to 6, but our results also indicate the efficacy of HAL rehabilitation for these patients ($d=.78$). Hornby et al¹¹ reported that after robotic-assisted locomotor training, the gait speed in chronic stroke patients increased by $.07 \pm .07$ m/s ($d=1.0$). Our results also indicate the efficacy of HAL rehabilitation for 9 patients with chronic stroke ($d=1.41$). We conjectured that the mechanism of this recovery of functional ambulation was due to changes in plasticity in the spinal cord and supraspinal centers. Appropriate sensory inputs, such as maximum weight loading, facilitating proper trunk posture, and hip extension, are essential for maximizing functional recovery.²² Our experience with HAL indicates that the HAL-induced motion might evoke the sensory input, which has a favorable feedback effect on the central nervous system for a recovery of locomotor function. In addition, even if a patient's condition were too severe for medical therapists to

provide adequate rehabilitation training, HAL might still make adequate training possible. HAL is a robotic device with potential rehabilitation applications that are dependent on the physical support it can provide.

Study limitations

This study was not a randomized controlled trial and could not compare the efficacy of HAL training with conventional rehabilitation. Second, long-term efficacy was not assessed after HAL training. Third, this study could not exclude observer bias and subject bias because the same staff implemented assessment and training, and approximately half of the patients were recruited through local newspaper advertisements. Finally, the statistical power was low because of the small number of patients with each disease.

Conclusions

This quasiexperimental study revealed the feasibility of HAL training for rehabilitating patients with limited mobility. This study has shown that it is possible to manage 8 weeks of rehabilitation with HAL training (16 sessions of 90min) safely and effectively, even with persons who received their diagnosis many years ago. After HAL training, significant improvements in gait speed, number of steps, and cadence were observed. Although improvements were observed in the TUG test and BBS, they were not statistically significant. There were no serious adverse events. Further studies are needed to compare the effectiveness of HAL training and conventional rehabilitation.

Suppliers

- Cyberdyne Inc, D25-1, Gakuen Minami, Tsukuba, Ibaraki, Japan 305-0818.
- ROPOX A/S, 221 Ringstedgade, Naestved, Denmark 4700.
- Biodex Medical Systems Inc, 20 Ramsay Rd, Shirley, NY 11967.
- SPSS, Inc, 233 S Wacker Dr, 11th Fl, Chicago, IL 60606.

Keywords

Feasibility studies; Mobility limitation; Orthopedic equipment; Rehabilitation; Robotics

Corresponding author

Kiyoshi Eguchi, MD, PhD, Associate Professor, Dept of Rehabilitation Medicine, Faculty of Medicine, University of Tsukuba, 1-1-1 Tennodai, Tsukuba, Ibaraki 305-8575, Japan. E-mail address: kyeguchi@md.tsukuba.ac.jp.

Acknowledgments

We thank Kanako Yamawaki, Ryohei Ariyasu, and Aki Ichikawa, Center for Cybernetics Research, University of Tsukuba, for their excellent technical assistance.

References

- van Vliet P, Wing AM. A new challenge: robotics in the rehabilitation of the neurologically motor impaired. *Phys Ther* 1991;71:39-47.
- Teferiller C, Pharo B, Evans N, Winchester P. Efficacy of rehabilitation robotics for walking training in neurological disorders: a review. *J Rehabil Res Dev* 2011;48:387-416.
- Colombo G, Joerg M, Schreiber R, Dietz V. Treadmill training of paraplegic patients using a robotic orthosis. *J Rehabil Res Dev* 2000;37:693-700.
- Veneman JF, Kruidhof R, Hekman EE, Ekkelenkamp R, Van Asseldonk EH, van der Kooij H. Design and evaluation of the LOPES exoskeleton robot for interactive gait rehabilitation. *IEEE Trans Neural Syst Rehabil Eng* 2007;15:379-86.
- Hesse S, Uhlenbrock D, Werner C, Bardeleben A. A mechanized gait trainer for restoring gait in nonambulatory subjects. *Arch Phys Med Rehabil* 2000;81:158-61.
- Schmidt H, Werner C, Bernhardt R, Hesse S, Kruger J. Gait rehabilitation machines based on programmable footplates. *J Neuroeng Rehabil* 2007;4:2.
- Vicintin M, Barbeau H, Komer-Bitensky N, Mayo NE. A new approach to retrain gait in stroke patients through body weight support and treadmill stimulation. *Stroke* 1998;29:1122-8.
- Lünenburger L, Colombo G, Rienen R, Dietz V. Biofeedback in gait training with the robotic orthosis Lokomat. *Conf Proc IEEE Eng Med Biol Soc* 2004;7:4888-91.
- Neckel N, Wisman W, Hilder J. Limb alignment and kinematics inside a Lokomat robotic orthosis. *Conf Proc IEEE Eng Med Biol Soc* 2006;1:2698-701.
- Husemann B, Müller F, Krewer C, Heller S, Koenig E. Effects of locomotion training with assistance of a robot-driven gait orthosis in hemiparetic patients after stroke: a randomized controlled pilot study. *Stroke* 2007;38:349-54.
- Hornby TG, Campbell DD, Kahn JH, Demott T, Moore JL, Roth HR. Enhanced gait-related improvements after therapist- versus robotic-assisted locomotor training in subjects with chronic stroke: a randomized controlled study. *Stroke* 2008;39:1786-92.
- Kawamoto H, Sankai Y. Power assist method based on phase sequence and muscle force condition for HAL. *Adv Robot* 2005;19:717-34.
- Lee S, Sankai Y. Virtual impedance adjustment in unconstrained motion for an exoskeletal robot assisting the lower limb. *Adv Robot* 2005;19:773-95.
- Suzuki K, Gouji M, Kawamoto H, Hasegawa Y, Sankai Y. Intention-based walking support for paraplegic patients with robot suit HAL. *Adv Robot* 2007;21:1441-69.
- Tsukahara A, Kawanishi R, Hasegawa Y, Sankai Y. Sit-to-stand and stand-to-sit transfer support for complete paraplegic patients with robot suit HAL. *Adv Robot* 2010;24:1615-38.
- Maeshima S, Osawa A, Nishio D, et al. Efficacy of a hybrid assistive limb in post-stroke hemiplegic patients: a preliminary report. *BMC Neuro* 2011;11:116.
- Michikawa T, Nishiwaki Y, Takebayashi T, Toyama Y. One-leg standing test for elderly populations. *J Orthop Sci* 2009;14(5):675-85.
- Berg K, Wood-Dauphinee S, Williams JJ. The balance scale: reliability assessment with elderly residents and patients with an acute stroke. *Scand J Rehabil Med* 1995;27:27-36.
- Nooljen CF, Ter Hoeve N, Field-Fote EC. Gait quality is improved by locomotor training in individuals with SCI regardless of training approach. *J Neuroeng Rehabil* 2009;6:36.
- Hachisuka K. [Robot-aided training rehabilitation] [Japanese]. *Brain Nerve* 2010;62(2):133-40.
- Wirz M, Zemon DH, Rupp R, et al. Effectiveness of automated locomotor training in patients with chronic incomplete spinal cord injury: a multicenter trial. *Arch Phys Med Rehabil* 2005;86:672-80.
- Barbeau H. Locomotor training in neurorehabilitation: emerging rehabilitation concepts. *Neurorehabil Neural Repair* 2003;17:3-11.

Feasibility and Safety of Acute Phase Rehabilitation After Stroke Using the Hybrid Assistive Limb Robot Suit

Tetsuya UEBA,¹ Omi HAMADA,¹ Toshiyasu OGATA,¹
Tooru INOUE,¹ Etsuji SHIOTA,² and Yoshiyuki SANKAI³

Departments of ¹Neurosurgery and ²Rehabilitation, Faculty of Medicine,
Fukuoka University, Fukuoka, Fukuoka;

³Center for Cybernetics Research, University of Tsukuba, Tsukuba, Ibaraki

Abstract

Acute phase rehabilitation is an important treatment for improving the functional outcome of patients after stroke. The present cohort study analyzed the feasibility and safety of acute phase rehabilitation using the hybrid assistive limb robot suit in 22 patients, 7 males and 15 females (mean age 66.6 ± 17.7 years). Neurological deterioration, mortality, or other accidents were recorded as adverse events. Baseline characteristics of each patient were recorded at the first hybrid assistive limb rehabilitation. Hybrid assistive limb rehabilitation was conducted for 12.1 ± 7.0 days with the patients in stable condition. Acute phase hybrid assistive limb rehabilitation was performed a total of 84 times with no adverse events recorded except for orthostatic hypotension. Good functional outcomes were obtained in 14 patients. Orthostatic hypotension was observed during the first hybrid assistive limb rehabilitation in four patients, and was significantly associated with intracerebral hemorrhage ($p = 0.007$) and lower Brunnstrom stage ($p = 0.033$). Acute phase rehabilitation using the hybrid assistive limb suit is feasible and safe. Patients with intracerebral hemorrhage and lower Brunnstrom stage should be carefully monitored for orthostatic hypotension.

Key words: acute phase rehabilitation, hybrid assistive limb robot suit, stroke, orthostatic hypotension

Introduction

Acute phase rehabilitation is an important part of the treatment for improving the functional outcome of patients after stroke in the acute hospital setting.^{3,5,6,8,9,13–15,17} The hybrid assistive limb (HAL) suit is one of a number of advanced technologies that have been developed for the assistance of stroke patients.^{12,16} This robotic device was originally designed to support elderly patients with muscle weakness, and to assist with independent mobility in people with impaired motor function. However, whether the HAL suit can be used for the rehabilitation of patients with acute stroke without adverse complications remains unclear. The present study investigated the feasibility and safety of the HAL suit in the rehabilitation of patients in the acute phase after stroke.

Materials and Methods

This prospective cohort study was designed to evaluate acute phase rehabilitation after stroke using the HAL robot suit in the Department of Neurosurgery, Fukuoka University Hospital from November 2011 to March 2012. A total of 22 patients, 7 males and 15 females (mean age 66.6 ± 17.7 years) were enrolled. The oldest participant was aged 90 years. The Fukuoka University Institutional Review Board approved the study and informed consent was obtained from all participants or their representatives. The protocol included subjects satisfying the following criteria: hemiplegia or ataxia after stroke, height > 120 cm, weight < 100 kg, Glasgow Coma Scale (GCS) score > 9 , systolic blood pressure between 100 and 160 mmHg, oxygen saturation without supplementation $> 90\%$, heart rate between 40 and 120 beats per minute, and body temperature $< 37.5^\circ\text{C}$. The limitations of height and weight were determined by the size restrictions of the HAL suit, as recommended by the manufacturer (CYBERDYNE

Inc., Tsukuba, Ibaraki). GCS score ≤ 9 was used to exclude coma status. Nine patients with subarachnoid hemorrhage, seven with intracerebral hemorrhage, and six with cerebral infarction were enrolled. Vital signs were carefully monitored during the rehabilitation. Anthropometry data, vital signs, time scheduled for HAL rehabilitation, time after eating, antihypertensive and diuretic medication, presence of diabetes mellitus, GCS, National Institute of Health Stroke Scale (NIHSS), Brunnstrom stage (Br), modified Rankin scale (mRS), mini-mental state examination (MMSE), presence of sensory disturbance, presence of neurocognitive impairment, disease entity (intracerebral hemorrhage, cerebral infarction, and subarachnoid hemorrhage), and adverse events including mortality, neurological deterioration, orthostatic hypotension (OH), fall, bone fracture, or skin erosion were recorded. OH was defined as a decrease in systolic blood pressure of over 20 mmHg immediately after sitting or standing.

Normally distributed data are expressed as mean \pm standard deviation. Age, systolic and diastolic blood pressure before HAL rehabilitation, time scheduled for HAL rehabilitation, time after eating, GCS, NIHSS, Br, mRS, and MMSE were treated as continuous variables. Sex, antihypertensive and diuretic medication, presence of diabetes mellitus, presence of sensory disturbance, presence of neurocognitive impairment, and clinical entity were treated as categorical variables. Fisher's exact test, t-test, and U-test were used to compare each variable and OH in the participants. Statistical differences of $p < 0.05$ were considered significant. Data analyses were performed using the SPSS 14.0.J program (SPSS Inc., Chicago, Illinois, USA).

Results

Acute phase rehabilitation using the HAL suit was performed a total of 84 times (mean 3.8 ± 3.1 times). HAL rehabilitation was conducted over 12.1 ± 7.0 days when the vital signs of the patients were stable (Fig. 1).

Following HAL rehabilitation, two patients had improved walking and torso posture, 12 patients could stand with HAL assistance, and two patients showed no change. Six patients withdrew from the study due to depression status, inappropriate size of shoes, and lumbar spondylosis, which prevented correct fitting of the backpack and mounting of the gyroscope and accelerometer required for torso posture estimation (Table 1).

No episode of mortality, neurological deterioration, falling, bone fracture, or skin erosion occurred

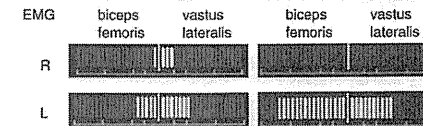
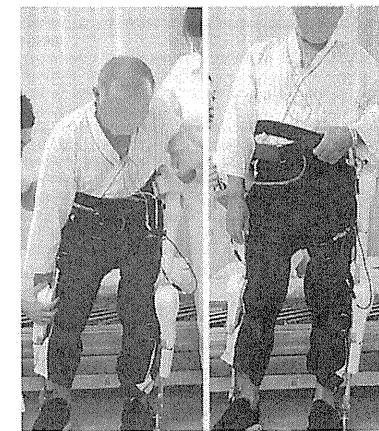


Fig. 1 Photographs during hybrid assistive limb (HAL) rehabilitation showing the patient in Brunnstrom stage II getting up (left) and standing upright (right) with HAL assistance. Electromyogram (EMG) was detected on the paralytic side while upright. L: left side, R: right side.

Table 1 Outcomes of hybrid assistive limb (HAL) training in stroke patients

Outcome	No. of cases
Improvement of walking and torso posture	2
Standing with HAL assist	12
No change in activity	2
Refusal of second HAL rehabilitation	6

throughout the acute phase rehabilitation using the HAL suit. However, four patients demonstrated OH as an adverse event, which prevented one patient receiving second HAL rehabilitation. Intracerebral hemorrhage and lower Br were significantly associated with OH, as demonstrated by Fisher's exact test and U-test ($p = 0.007$ and $p = 0.033$, respectively; Table 2). No other variables were associated with OH (Table 2). Lower Br was not associated with any of the clinical characteristics (Kruskal Wallis test, $p = 0.266$).

Table 2 Factors correlated with orthostatic hypotension

Factors	Orthostatic hypotension		p Value
	No	Yes	
No. of patients	18	4	
Age (yrs)	66.0 (19.0)	69 (12.2)	0.772
Sex, men/women	6/12	1/3	1.000
Body mass index	21.2 (4.8)	21.0 (4.0)	0.953
Pre-HAL systolic BP (mmHg)	130.9 (20.8)	129.5 (18.5)	0.900
Pre-HAL diastolic BP (mmHg)	73.4 (13.2)	86.3 (12.8)	0.092
Time scheduled for HAL (hrs)	2:00 PM	1:00 PM	0.218
Time after eating (hrs)	3.5 (1.3)	3.0 (0.4)	0.220
Antihypertensive medication	13	9	0.264*
Diuretic medication	21	1	1.000*
Diabetes mellitus	19	3	0.470*
GCS score	14.1 (1.6)	12.5 (1.9)	0.102
NIHSS score	6.9 (7.9)	14.8 (13.9)	0.094
Brunnstrom stage	4.1 (1.6)	2.0 (2.0)	0.033
MMSE point	17.8 (11.2)	11.5 (13.9)	0.338
Modified Rankin scale score	4.0 (2-5)	4.8 (0.5)	0.082†
Presence of sensory disturbance	13	3	1.000*
Presence of neurocognitive impairment	11	3	1.000*
First HAL rehabilitation day	12.7 (7.6)	9.5 (2.4)	0.426
Times of HAL rehabilitation performed	3.5 (2.4)	5.3 (5.7)	0.585
Disease entity			0.007*
subarachnoid hemorrhage	9	0	
intracerebral hemorrhage	3	4	
cerebral infarction	6	0	

Values in normal distribution are shown as the mean (standard deviation), and values in non-normal distribution are shown as the median (minimum-maximum). All variables were recorded on the first day of HAL rehabilitation. p Values are calculated by t-test, *Fischer's exact test, or †U-test. BP: blood pressure, GCS: Glasgow Coma Scale, HAL: hybrid assistive limb, MMSE: mini-mental state examination, NIHSS: National Institute of Health Stroke Scale.

Discussion

The present study demonstrated that HAL rehabilitation is feasible and safe after stroke in the acute phase. To prevent falls, neurological deterioration, or any other morbidity, the presence of OH should be monitored in patients with intracerebral hemorrhage and lower Br. An elastic stocking on the paralytic side or delaying rehabilitation for a few days enabled us to continue HAL rehabilitation in three of four patients with OH. OH has been attributed to the time after eating, antihypertensive and diuretic medications, and the presence of diabetes mellitus, implying the involvement of autonomic dysfunction.¹⁰ However, we found no significant differences in these variables between the patients with and without OH, as only intracerebral hemorrhage

and lower Br were significantly associated with OH. Lower Br was not associated with any clinical characteristic, suggesting that intracerebral hemorrhage and lower Br were not confounding factors. The variable of intracerebral hemorrhage may be an independent risk factor for OH. The severe degree of autonomic dysfunction in patients with intracerebral hemorrhage is a likely mechanism of OH in the present acute setting. Further studies with more cases are required to avoid type II error.

The HAL suit consists of a 'cybernetic voluntary control system,' which provides complete control using bioelectric signals, and a 'cybernetic robotic autonomous control system,' which generates the characteristic motor patterns of human motion.^{12,19} The HAL system functions by utilizing several sensing modalities: skin-surface electromyographic electrodes placed on the rectus femoris, vastus lateralis, gluteus maximus, and biceps femoris muscles, potentiometers, and a gyroscope and accelerometer mounted in a backpack for torso posture estimation. The objective of the HAL suit is to increase and assist the voluntary motor functions of stroke patients. We found that some patients exhibited electric signals on the paralytic side, which might have been facilitated by the HAL suit (Fig. 1). Standing with assistance of the HAL suit in the acute phase may not only facilitate the recovery of the paralytic side, but also prevent the non-paralytic side from disuse, allowing patients to have a better quality of life. Indeed, a prospective study reported that earlier and more intensive mobilization after stroke may facilitate more rapid return to unassisted walking and improve functional recovery.⁹ We expect that HAL acute phase rehabilitation will also result in earlier and better recovery. Standing and walking are also reported to induce plasticity in the spinal cord network and central pattern generator.⁷

Age,² depression,⁴ and cognitive impairment¹¹ are potential negative factors hindering good functional outcomes. In this feasibility study, depression was the main reason for the refusal of HAL rehabilitation. Furthermore, particular attention should be paid to the presence of OH which can induce falls¹⁰ and result in serious consequences.¹ The efficacy and indications of acute phase rehabilitation using HAL are being examined in a follow-up cohort study.

Acknowledgments

The patient and physical therapist provided written informed consent for the use of the photograph in Fig. 1.

Conflicts of Interest Disclosure

None declared. All authors who are members of The Japan Neurosurgical Society (JNS) have registered online Self-reported COI Disclosure Statement Forms through the website for JNS members.

References

- 1) Batchelor FA, Mackintosh SF, Said CM, Hill KD: Falls after stroke. *Int J Stroke* 7: 482-490, 2012
- 2) Béjot Y, Rouaud O, Jacquin A, Osseby GV, Durier J, Manckoundia P, Pfitzenmeyer P, Moreau T, Giroud M: Stroke in the very old: incidence, risk factors, clinical features, outcomes and access to resources—a 22-year population-based study. *Cerebrovasc Dis* 29: 111-121, 2010
- 3) Bernhardt J, Dewey H, Thrift A, Collier J, Donnan G: A very early rehabilitation trial for stroke (AVERT): phase II safety and feasibility. *Stroke* 39: 390-396, 2008
- 4) Carod-Artal FJ, Ferreira Coral L, Trizotto DS, Menezes Moreira C: Poststroke depression: prevalence and determinants in Brazilian stroke patients. *Cerebrovasc Dis* 28: 157-165, 2009
- 5) Chan DK, Cordato D, O'Rourke F, Chan DL, Pollack M, Middleton S, Levi C: Comprehensive stroke units: a review of comparative evidence and experience. *Int J Stroke* Epub 2012 Jul 19
- 6) Cumming TB, Thrift AG, Collier JM, Churilov L, Dewey HM, Donnan GA, Bernhardt J: Very early mobilization after stroke fast-tracks return to walking: further results from the phase II AVERT randomized controlled trial. *Stroke* 42: 153-158, 2011
- 7) Dietz V: Proprioception and locomotor disorders. *Nat Rev Neurosci* 3: 781-790, 2002
- 8) Di Lauro A, Pellegrino L, Savastano G, Ferraro C, Fusco M, Balzarano F, Franco MM, Biancardi LG, Grasso A: A randomized trial on the efficacy of intensive rehabilitation in the acute phase of ischemic stroke. *J Neurol* 250: 1206-1208, 2003
- 9) Drummond AE, Pearson B, Lincoln NB, Berman P: Ten year follow-up of a randomised controlled trial of care in a stroke rehabilitation unit. *BMJ* 331: 491-492, 2005

- 10) Feldstein C, Weder AB: Orthostatic hypotension: a common, serious and underrecognized problem in hospitalized patients. *J Am Soc Hypertens* 6: 27-39, 2012
- 11) Jaillard A, Grand S, Le Bas JF, Hommel M: Predicting cognitive dysfunctioning in nondemented patients early after stroke. *Cerebrovasc Dis* 29: 415-423, 2010
- 12) Kawamoto H, Taal S, Niniss H, Hayashi T, Kamibayashi K, Eguchi K, Sankai Y: Voluntary motion support control of Robot Suit HAL triggered by bioelectrical signal for hemiplegia. *Conf Proc IEEE Eng Med Biol Soc* 2010: 462-466, 2010
- 13) Kwakkel G, Wagenaar RC, Koelman TW, Lankhorst GJ, Koetsier JC: Effects of intensity of rehabilitation after stroke. A research synthesis. *Stroke* 28: 1550-1556, 1997
- 14) Kwakkel G, Wagenaar RC, Twisk JW, Lankhorst GJ, Koetsier JC: Intensity of leg and arm training after primary middle-cerebral-artery stroke: a randomised trial. *Lancet* 354: 191-196, 1999
- 15) Langhorne P, Stott D, Knight A, Bernhardt J, Barer D, Watkins C: Very early rehabilitation or intensive telemetry after stroke: a pilot randomised trial. *Cerebrovasc Dis* 29: 352-360, 2010
- 16) Maeshima S, Osawa A, Nishio D, Hirano Y, Takeda K, Kigawa H, Sankai Y: Efficacy of a hybrid assistive limb in post-stroke hemiplegic patients: a preliminary report. *BMC Neurol* 11: 116, 2011
- 17) Preston E, Ada L, Dean CM, Stanton R, Waddington G: What is the probability of patients who are nonambulatory after stroke regaining independent walking? A systematic review. *Int J Stroke* 6: 531-540, 2011
- 18) Tang A, Eng JJ, Krassioukov A: Application of the Sit-Up Test for orthostatic hypotension in individuals with stroke. *Auton Neurosci* 168: 82-87, 2012

Address reprint requests to: Tetsuya Ueba, MD, PhD, Department of Neurosurgery, Faculty of Medicine, Fukuoka University, 7-45-1 Nanakuma, Jonan-ku, Fukuoka 814-0180, Japan.
e-mail: tueba@fukuoka-u.ac.jp

Measurement method of interaction force between human and wearable assistive robot based on strain of contact part

Minh Tuan Nguyen¹ and Yoshiyuki Sankai¹

¹Department of Intelligent interaction technologies, University of Tsukuba. 1-1-1 Tennodai, Tsukuba, Japan
(E-mail: {nguyen, sankai}@golem.kz.tsukuba.ac.jp)

Abstract: In order not only to realize the functions of wearable robots, but also to improve the design of mechanism and controller, and to establish a safety standard of these types of robots, a method to measure the physical interaction at the contact sites of robot and wearer is required. To evaluate the physical interaction, we propose a measurement method based on strain gauge. A basic experiment was conducted to evaluate the proposed method. The proposed method is also applied to Robot Suit HAL for Well-being to evaluate its interaction with a wearer during several kinds of single joint motion task. Experimental results show the plausibility of this approach for the measurement of the interaction force.

Keywords: exoskeleton, human-machine interaction, motion assist, force measurement

1. INTRODUCTION

Wearable robots, which support, enhance and extend human physical capabilities, are expected to be used for various kinds of purposes, by incorporating adaptability of computer programming and physical strength of mechanical structures[1]. In the field of medical care and welfare, wearable robots are expected to support physically challenged persons so that they can, for example, eat[2] and locomote[3] independently. In rehabilitation of the impaired motions, they are expected to assist motions of the affected limbs, as well as helping physical therapists from repeating many times the burdensome exercises for functional recovery[4]. Nowadays, interactive bio-feedback loop of motion intention and execution and resultant sensation realized by a wearable robot is thought to be able to play an important role in the neural recovery of the impaired motions[5]. Care givers may also have benefit wearing these robots in carrying and moving the patients[6].

Wearable robots assist motions by applying forces directly on the wearers body[1]. When they push or pull each other, interaction force between them are caused at the contact sites. Measuring interaction force provides a criteria to evaluate the effectiveness of assist given by the robot to the wearer, and to evaluate usability, comfort, and safety from the wearer's viewpoint. This gives critical information to improve the design of mechanism and controller[7]. It may also lead to establishment of a safety standard for these types of robots, which is needed since wearable robots are abundantly developed and even already used in some clinical situations.

Cuff accompanied with stretching belt is one of the major methods of mounting robot to human body, since it is adaptive to the shape of human leg and lessens peak pressure by widening contact areas. Cuff is used for example in HAL[8], LOPES[9], Locomat[4], etc.

In human biomechanics, each body segment is considered as a rigid body, and motion of it is determined by the total force acting on it according to the Newton's law. Likewise in evaluation of the effectiveness of assist and support provided by the robot, total force on each body

segment gives the most direct value related to the resulting motion. Therefore, we are interested in the amount and direction of total force at each cuff, instead of pressure at each point in the contact area. De Rossi et al. [10] has proposed tactile sensors (Skilsens) to measure the interaction force at the cuff of LOPES, however it can measure only component of the forces perpendicular to the sensor surface. There are some proposed methods using load cells[11][8], they measure load on robot structure rather than interaction force at the contact site.

In this paper, we propose a method to measure interaction force between robot and human body using strain gauges installed on the metal frame of cuff. To restrict the number, location, and direction of the forces applied on the metal frame, we propose to introduce load bearings of the same number of the strain gauge pairs into the gap between the metal frame and the contacting surface. In section II, our target robot HAL is briefly depicted. In section III, installation of strain gauges and bearings, model of strain-force relationship, and its calibration is described. In section IV, a basic experiment to evaluate the plausibility of the obtained forces is shown. In section V, the paper is concluded.

2. HAL (HYBRID ASSISTIVE LIMBS)

Robot suit HAL for well-being (Fig.1) is developed for the purpose of assisting motions of neurologically impaired persons[5][12]. It is composed of power units to actuate the hip and knee joints on both sides, exoskeleton frame to transfer actuation and to support the wearer's posture, and several sensors including joint angle sensors, floor reaction force sensors, and current sensor for each motor.

HAL has two modes of assistive control; CAC (Cybernetic Autonomous Control) and CVC (Cybernetic Voluntary Control). According to situation of the patient, one or combination of them is applied. In CVC mode, HAL provides assist according to the bio-electric signal detected on the surface of the skin, which represents the wearer's intention to activate muscle. This method is useful for augmenting or supporting healthy and lightly impaired

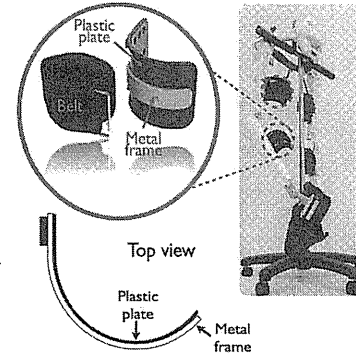


Fig. 1 HAL for well-being and its cuff: the cuff is structured with a metal frame and a plastic plate, and attached to the robot frame. A belt is used to wrap around them and human leg.

person's motion. CAC mode is for spinal cord injury patients and stroke patients whose motor center of nervous system is damaged and bio-electric signal cannot be detected. In this mode, HAL utilizes floor reaction force and accelerometers to estimate the intention of motion, and presents pre-planned trajectory.

Cuff of HAL is used to contact thigh and shank of the wearer to the robot frame for the left and right legs. Its structure, as shown in Fig.1, has a plastic frame that interfaces with human leg through a thin sponge on it and a metal frame which keeps the curved shape while bearing the interaction force. They are attached to the robot frame which transmits motor actuation. The metal frame is bonded between the plastic frame and the robot frame. A stretching belt is used to wrap around human leg and the cuff. Strain gauges are attached to measure the bending of the metal frame, as will be described in the next section.

3. METHOD

3.1 Model of Cuff Strain - Force Relationship

On a thin cantilevered curved beam, when the thickness is enough smaller than than the radius of the whole shape, the relation among the bending component of strain ϵ , which can be obtained by the subtraction between the measured strain on one side (ϵ_a) and the other side (ϵ_b)

$$\epsilon = \epsilon_a - \epsilon_b, \quad (1)$$

the applied external force \vec{F} , and the vector \vec{l} starting from the position of strain gauges to the point where the force is applied, is given by the following equation

$$C\epsilon = \vec{l} \times \vec{F}. \quad (2)$$

C is a constant representing the local properties of shape and material characteristics. Strain ϵ is given by the subtraction between the two strains measured on two opposite sides at a location on the beam.

Supposing that we have n pairs of strain gauges and m forces applied on the beam,

$$C_i \epsilon_i = M_i \quad (i = 1 \cdots n) \quad (3)$$

$$M_i = \sum_{j \in q(i)} \vec{l}_{ij} \times \vec{f}_j, \quad (4)$$

where M_i represents total bending moment working on the i th strain gauge pair and $q(i)$ represents the set of forces that can apply bending moment at i th strain gauges. Outer product $\vec{l}_{ij} \times \vec{f}_j$ is equal to the scalar product of d_{ij} and f_j

$$M_i = \sum_{j \in q(i)} d_{ij} f_j, \quad (5)$$

where d_{ij} is a perpendicular distance between the location of strain gauges and the force vector crossing the applied point, and f_j is the amplitude of the force.

By arranging the indexes in eq.(5) and considering eq.(3), we can get the following matrix representation.

$$C\epsilon = Df, \quad (6)$$

where C is a diagonal matrix with C_i in the diagonal components, ϵ is a vector composed of ϵ_i , D is a matrix composed of d_{ij} considering $q(i)$, and f is a vector composed of f_j . In practice, values of strain is affected by the weight of the beam and initial state of the gauges in attachment, which should be counted as an offset b ,

$$C\epsilon - b = Df \quad (7)$$

By designing the location of strain gauges so that D is invertible, the interaction forces f can be obtained as,

$$f = D^{-1}(C\epsilon - b) \quad (8)$$

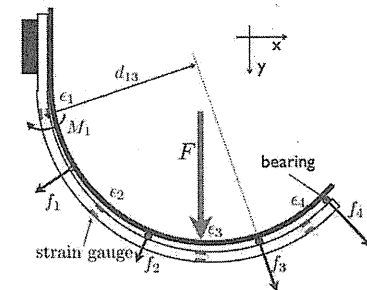


Fig. 2 Placement of strain gauges and load bearings on a cuff of robot suit HAL.

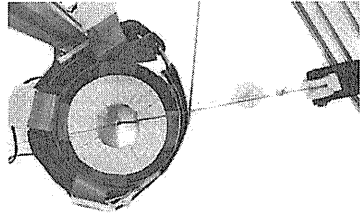


Fig. 3 Setup in the calibration experiment.

In calibration process, values of strain are obtained corresponding to the known applied forces. Using these values, coefficients of eq.(8) can be computed by regression. Knowing the coefficients, the equation can be used to estimate the applied forces according to the measured strains.

However, on cuff of wearable robots, because of the flexible interface with the human leg like plastic plates and sponges, the forces are scattered all over the interfacing surface, and it is difficult to assume the number, direction, and applied points of the forces. To deal with this problem, we would install load bearings between the metal frame and the plastic plate, in the next subsection.

3.2 Installing Strain Gauges onto Cuff

For the derivation in the previous subsection to hold, the number, direction, and applied points of the forces on the metal frame, on which the strain gauges are attached, have to be known. For this reason we introduced four load bearings between the metal frame and the plastic plate of a cuff of HAL (Fig.2). In this way, the number of the forces acting on the metal frame are restricted to be the same number as the bearings, the direction is restricted to be perpendicular to the metal frame, and the applied points are restricted to be same as the attachment points of the bearings. By this way, we can apply eq.(8).

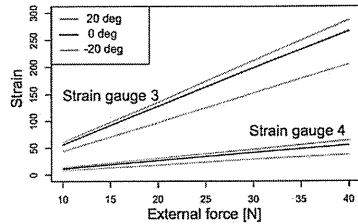


Fig. 4 Linear relationship between the applied external force and the strain. The external forces are applied with various amplitude and direction.

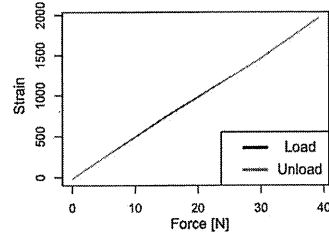


Fig. 5 Hysteresis test to compare the change of strain with the increasing and decreasing external loads.

As we have discussed in the introduction, we are interested in measurement of total force acting between the human leg and the robot through cuff. Since we have introduced four bearings, the total force F is computed as

$$F = \vec{f}_1 + \vec{f}_2 + \vec{f}_3 + \vec{f}_4 \quad (9)$$

By introducing the coordinate frame (x, y) shown in Fig.2, \vec{f}_i can be written in x and y components.

$$\vec{f}_i = [t_{ix}, t_{iy}]^T f_i \quad (10)$$

Considering eqs.(9), (10), and (8), we have

$$F = Tf \quad (11)$$

$$= TD^{-1}C\epsilon - TD^{-1}b \quad (12)$$

$$= A\epsilon - b', \quad (13)$$

where T is a matrix with t_{ix} and t_{iy} in the components, and A and b' are simplified representation of the coefficients. It shows that the total force F and the bending strains ϵ have a simple relationship represented by a linear coefficient matrix with an offset vector. These coefficients will be calibrated in a basic experiment in the next section.

Before calibration of the parameters, several basic characteristics of the strain were tested. Fig.4 shows linearity between the applied external force and the bending

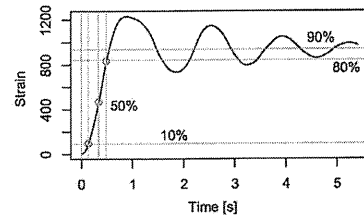


Fig. 6 Step response of the strain.

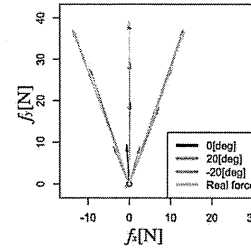


Fig. 7 Result of calibration: estimated forces can be compared to the real forces. Top: pushing direction. Bottom: pulling direction.

component of the measured strain value (eq.(1)). The angles of the external force conform to the definition in the next section.

Fig.5 shows the result of hysteresis test, in which the external force was gradually increased and then decreased with the interval of 0.5[kg]. It shows that there is no significant hysteresis in the strain value, which allows simple mapping of the strain values to estimate force.

Fig.6 shows step response of the strain value to the external force. 3[kg] load was initially applied and at one moment it was reduced to 1[kg]. In the graph, the value of strain is normalized to 0 initial value, and the amount of change to positive. It shows that the response is fast enough for our purpose of measuring human walking or leg swinging.

3.3 Calibration of the Model

To calibrate the parameters A and b' in eq.(13) the cuff was attached to a soft cylinder which mimics human leg, and external forces were applied by pulling the cylinder into several directions at several amplitudes (Fig.3).

Parameters of the applied forces were 1.amplitude (from 0[N] to 40[N] with 10[N] interval), 2. direction (pulling and pushing the metal frame), 3. angle (0[deg], 20[deg], -20[deg]). These parameters were applied to each channel, therefore generating $5 \times 2 \times 3 \times 4 = 120$ sets of data. Among the 120 sets randomly chosen 80 sets

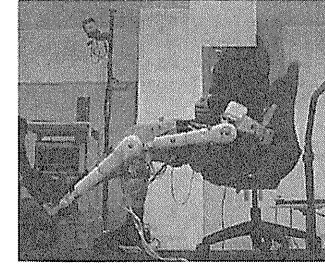


Fig. 8 Single joint experiment with HAL. HAL and the wearer swing the knee joint and the interaction force at the shank cuff is measured.

were used for regression, and the resting 40 sets were used to test the calibration.

The result is shown in Fig.7. The estimated forces are enough close to the given force shown in gray arrow, in both of the pushing (Left) and pulling (Right) direction. Statistically, in the pushing direction, 95% of the error was less than 1.7[N] and 2.5[deg], and in the pulling direction, it was less than 4[N] and 4.3[deg]. We suspect that the cause of the difference in the directions may be the structural difference. For example, the curvature of cuff is different between the directions, a plastic plate is attached only on the inner side of the metal part, and a belt wraps around the metal part. It has to be investigated into more detail in future.

4. EXPERIMENT

We tested the plausibility of the estimated interaction force in a situation where a human wears HAL. For this purpose, single joint motion, where the wearer (one healthy subject) sits on a chair wearing HAL and moves his left lower leg around the knee joint, was tested (Fig.8). Control mode of HAL was either fully autonomous, no actuation, viscosity compensation or CVC (c.f. section 2). In the fully autonomous mode, it was controlled to track a pre-planned sine wave trajectory of 0.5[Hz] with 45[deg] amplitude at the knee joint with a comparatively high feedback gain. In this control mode, the wearer was asked to swing his leg in accordance with the HAL motion, earlier than HAL as if to increase the pace of swinging, or later than HAL as if to decrease the pace. In the other control modes the wearer was asked to swing his leg according to a metronome ringing at 0.5[Hz]. We referred to [13] to design the experiment.

Fig.9 shows knee joint angle, its velocity and the estimated interaction force at the shank cuff. Larger joint angle indicates flexing and positive force indicates pushing (ex. HAL pushes human leg into extension). In the case where the wearer tries to swing earlier than HAL (Top Left), the interaction force is almost in phase with the velocity reflecting that the wearer is trying to accelerate HAL. Contrarily, in the opposite case (Top Right),

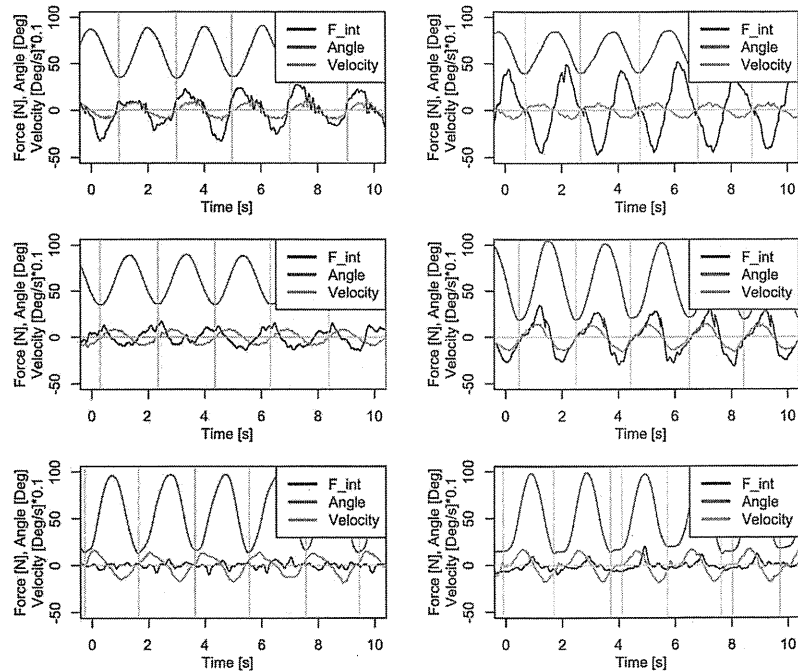


Fig. 9 Knee joint angle, its velocity and the interaction force at the shank cuff. Larger joint angle indicates flexion and positive force indicates pushing (ex. HAL pushes human leg into extension). Top Left: Autonomous control. Wearer tries to swing earlier than HAL as if to increase pace. Top Right: Autonomous control. Wearer tries to swing later than HAL as if to decrease pace. Middle Left: Autonomous control. Wearer tries to swing in accordance with HAL. Middle Right: No actuation. Wearer swings according to the metronome. Bottom Left: Viscosity compensation control. Wearer swings according to the metronome. Bottom Right: CVC mode. Wearer swings according to the metronome.

the force is almost anti-phase with the velocity, since the wearer is trying to decelerate HAL. In the case of no actuation (Middle Right), the force is almost in-phase with the velocity, since the wearer has to exert against mechanical viscosity. In the other three cases, interaction force was comparatively small, reflecting the nature of the motions. It is interesting to see that with a healthy subject viscosity compensation control and CVC do not make much differences in amplitude, since his bio-electric signal and motion is almost synchronized.

Compared to the joint angle and velocity trajectories which seem to be resembling to each other among the various control conditions, which is natural after the task was to swing the lower limb at the same frequency and amplitude, the interactive force varies a lot. It implicates the importance of measuring the interaction force directly. For example, inverse dynamics method which computes

the interactive force based on kinematic movement is not appropriate to uncover such variation, since the interactive force may not appear in joint motion by being balanced with joint torques of human skeleton and HAL. Simply put, it is possible that the human leg and HAL pushing or pulling strongly each other, but still keeping a static situation. Also, as shown in the results, HAL may be assisting or preventing the motion of the human leg, which is very important in evaluating the role of motion assistive robots.

In this experiment, a simple task of single joint motion was conducted to evaluate the plausibility of the method. It was adopted as a test motion because it allows intuitive interpretation of the estimated forces. At the same time, this motion has clinically significant implication. In the treatment course of rehabilitation after damage caused by stroke or other neural or biomechanical injuries, patients

first go through training of single joint motions lying on a bed or seated on a chair, before going into the stage of walking training. Since the robot assisted rehabilitation is expected to be applicable to the single joint training as well as walking training, data obtained in this section has possibility to provide reference for evaluation of clinical single joint training in a future perspective.

5. CONCLUSION

We proposed a method to measure the interaction force between human and wearable robot based on strain gauges installed on cuff frame. By this method, total force of interaction at cuff can be measured at a good accuracy, without affecting the interaction, whose plausibility was shown in a single joint motion experiment with HAL and a human wearer. Future work includes application to locomotion support and analysis of effectiveness of assist and safety.

ACKNOWLEDGMENTS

This research was supported by NEDO project. Authors thank Pr.Hideki Kadone, Pr.Hiroaki Kawamoto, and Dr.Cota Nabeshima for valuable comments.

REFERENCES

- [1] J.L. Pons. *Wearable robots: biomechatronic exoskeletons*, volume 70. Wiley Online Library, 2008.
- [2] Y. Hasegawa and S. Oura. Exoskeletal meal assistance system (emas ii) for progressive muscle dystrophy patient. In *Rehabilitation Robotics (ICORR), 2011 IEEE International Conference on*, pages 1 – 6, 29 2011-july 1 2011.
- [3] Katherine A. Strausser and H. Kazerooni. The development and testing of a human machine interface for a mobile medical exoskeleton. In *Intelligent Robots and Systems (IROS), 2011 IEEE/RSJ International Conference on*, pages 4911 –4916, sept. 2011.
- [4] A. Mayr, M. Kofler, E. Quirbach, H. Matzak, K. Frhlich, and L. Saltuari. Prospective, blinded, randomized crossover study of gait rehabilitation in stroke patients using the lokomat gait orthosis. *Neurorehabilitation and Neural Repair*, 21(4):307–314, 2007.
- [5] Yoshiyuki Sankai. *HAL: Hybrid Assistive Limb Based on Cybernetics*, volume 66 of *Springer Tracts in Advanced Robotics*, chapter 3, pages 25–34. Springer Berlin Heidelberg, 2011.
- [6] H. Satoh, T. Kawabata, and Y. Sankai. Bathing care assistance with robot suit hal. In *Robotics and Biomimetics (ROBIO), 2009 IEEE International Conference on*, pages 498–503.
- [7] Y. H. Yin, Y. J. Fan, and L. D. Xu. Emg and epp-integrated human machine interface between the paralyzed and rehabilitation exoskeleton. *Information Technology in Biomedicine, IEEE Transactions on*, 16(4):542–549, 2012.
- [8] T. Hayashi, H. Kawamoto, and Y. Sankai. Control method of robot suit hal working as operator's muscle using biological and dynamical information. In *Intelligent Robots and Systems, 2005. (IROS 2005). 2005 IEEE/RSJ International Conference on*, pages 3063–3068.
- [9] J. F. Veneman, R. Kruidhof, E. E. G. Hekman, R. Ekkelenkamp, E. H. F. Van Asseldonk, and H. van der Kooij. Design and evaluation of the lopes exoskeleton robot for interactive gait rehabilitation. *IEEE Transactions on Neural Systems and Rehabilitation Engineering*, 15(3):379–386, 2007. 212JU Times Cited:86 Cited References Count:26.
- [10] S. M. De Rossi, N. Vitiello, T. Lenzi, R. Ronssse, B. Koopman, A. Persichetti, F. Vecchi, A. J. Ijspeert, H. van der Kooij, and M. C. Carrozza. Sensing pressure distribution on a lower-limb exoskeleton physical human-machine interface. *Sensors (Basel)*, 11(1):207–27, 2011.
- [11] C.J. Walsh, K. Endo, and H. Herr. A quasi-passive leg exoskeleton for load-carrying augmentation. *International Journal of Humanoid Robotics*, 4(03):487–506, 2007.
- [12] H. Kawamoto, S. Taal, H. Niniss, T. Hayashi, K. Kamibayashi, K. Eguchi, and Y. Sankai. Voluntary motion support control of robot suit hal triggered by bioelectrical signal for hemiplegia. In *Engineering in Medicine and Biology Society (EMBC), 2010 Annual International Conference of the IEEE*, pages 462–466.
- [13] Tommaso Lenzi, Nicola Vitiello, Stefano Marco Maria De Rossi, Alessandro Persichetti, Francesco Giovacchini, Stefano Roccella, Fabrizio Vecchi, and Maria Chiara Carrozza. Measuring humanrobot interaction on wearable robots: A distributed approach. *Mechatronics*, 21(6):1123–1131, 2011.

Exoskeletal Neuro-Rehabilitation in Chronic Paraplegic Patients – Initial Results

Mirko Aach^{1,*}, Renate Meindl¹, Tomohiro Hayashi^{1,4}, Irene Lange¹, Jan GeBmann¹, Andre Sander¹, Volkmar Nicolas³, Peter Schwenkreis², Martin Tegenthoff², Yoshiyuki Sankai^{1,4}, and Thomas A. Schildhauer^{1,*}

¹ Department of General and Trauma Surgery, BG University Hospital Bergmannsheil, Ruhr-University Bochum, Germany
{mirko.aach,schildhauer}@bergmannsheil.de

² Department of Neurology, BG University Hospital Bergmannsheil, Ruhr-University Bochum, Germany
{peter.schwenkreis,martin.tegenthoff}@bergmannsheil.de

³ Department of Radiology, BG University Hospital Bergmannsheil, Ruhr-University Bochum, Germany
volkmar.nicolas@bergmannsheil.de

⁴ Cyberdyne Inc., Institute of Engineering, Mechanics and Systems, University of Tsukuba, Japan
sankai@cyberdyne.jp

Abstract. Treadmill training after traumatic spinal cord injury is established as a therapy to improve walking capabilities in incomplete injured patients. In this study we investigate walking capabilities after a three month period of HAL[®] exoskeleton supported treadmill training in patients with chronic (>6 month) complete/incomplete (ASIA A – ASIA C) spinal cord injury. We monitored walking distance, walking speed and walking time with additional analysis of functional improvement by using the 10-m-walk test, the timed-up-and-go test and the WISCI II score in combination with the ASIA classification.

1 Introduction

Previous studies have confirmed that regular treadmill training can improve walking capabilities in incomplete spinal cord injury patients [1-4]. Over the last ten years,

1 Introduction

Previous studies have confirmed that regular treadmill training can improve walking capabilities in incomplete spinal cord injury patients [1-4]. Over the last ten years, driven gait orthoses have been applied for such treadmill training in order to move the patient's legs continuously and physiologically [5-7]. However, such training requires extensive resources, is locally limited to the treadmill, does not allow supported walking abilities outside the driven gait orthoses attached to the treadmill, and is limited only to passive motion of the legs. More recently, various exoskeleton systems for paraplegic patients became available, which allow patient mobilization outside the treadmill, though, mainly on a basis of passive range of motion (ROM).

* Corresponding authors.

The HAL[®] Robot Suit (Cyberdyne Inc. Japan) however, additionally allows voluntary machine supported active ROM (CVC mode) of incomplete paraplegic patients by using minimal bioelectric signals recovered from hip and knee flexors and extensors [8-10]. The goal of this study is to evaluate initial functional results in chronically complete/incomplete paraplegic patients after using the supported active ROM mode of the HAL[®] Robot Suit Exoskeleton.

2 Material and Methods

2.1 Subjects

We have investigated four patients (35 years to 62 years of age; 3 males and 1 female) with chronic (time since injury > 6 months) paraplegic spinal cord injury participated in the HAL[®] Robot Suit training for a three months period. One patient suffered from incomplete thoracic spinal cord injury (ASIA C), two patients from an incomplete lesion of the conus medullaris / cauda equine (ASIA B/C), and one complete paraplegic patient below Th 12 with zones of partial preservation in L1-L3 (ASIA A).

2.2 Treadmill Associated Measurements

Walking distance, walking speed and walking time when wearing the robot suit were measured on the treadmill at the beginning of the training, as well as after 6 and 12 weeks. Also the body weight support was measured.

2.3 Functional Measurements

To describe the functional improvement we did the 10-m-walk test before and after each training. The timed-up-and-go test was done once a week. By using the WISCI II score the needed support was documented.

2.4 Others

Additionally we measured individual spasticity of one patient with the modified Ashworth scale. The muscle strength according to the Frankel scale was recorded although as the ASIA score.

3 Results

During the training period, initial body weight support when wearing the HAL[®] robot suit could be reduced from 30% body weight to 15% (3 patients) and 0% (1 patient) of body weight. The walking distance when wearing the robot suit with voluntary machine supported active motion (CVC mode) increased significantly from 62 m – 216 m to 260 m – 1153 m after three months of training (as shown in Fig.1).

Ashworth scale. The muscle strength according to the Frankel scale was recorded

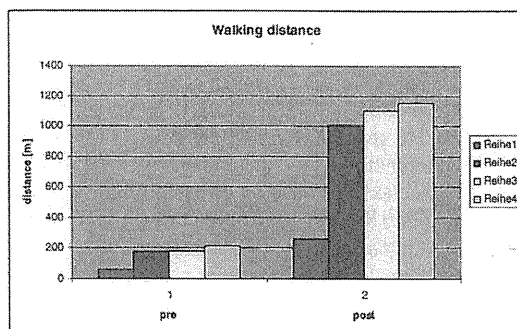


Fig. 1 Walking distance in pre and post evaluation

The walking speed increased from 0.7 km/h up to 2.2 – 2.8 km/h. Only one patient with spasticity had no improvement.

The walking time increased also from 12.09 – 18.14 min. to 18.01 – 30.03 min.

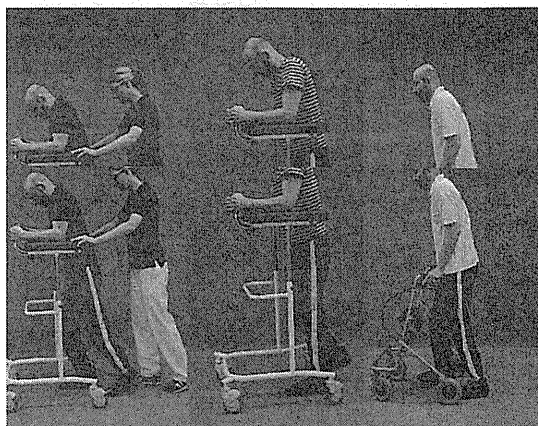
The needed time for the 10-m-walk test was significantly reduced in three patients from 56.82 – 72.02 sec. to 16.50 – 27.44 sec.

All patients showed reduction of the needed time for the timed-up-and-go test (31.22 – 82.03 sec. to 34.22 sec. – 74.06 sec.)

After the HAL[®] exoskeleton training the spasticity in one patient was reduced from Ashworth IV to Ashworth II.

Two patients were able to reduce the support in the 10-m-walk test, measured with the WISCI II score. The score increased from 6 to 9 points after 12 weeks (as shown in Fig. 2).

One patient (date of injury 25.05.2011) switched from ASIA B (24.02.2012) to ASIA C (05.06.2012). In the other patients we found no significant increase in muscle strength.



4 Discussion

Our preliminary results present in all patients significant increases in their functional abilities already after a three months period of active training using the HAL[®] robot suit in a CVC mode. Not only the treadmill associated walking and the on ground walking increased. Although an improvement in the WISCI II score and a switch in the ASIA classification were shown in some patients. These results have to be evaluated against the background that all patients were chronic spinal cord injured and were already on a constant functional level after intensive standard neuro-rehabilitation training.

5 Conclusion

Treadmill training using the HAL[®] exoskeleton might be a useful innovative training in chronic SCI-patients. However, these promising preliminary results are only descriptive and must be confirmed in a larger group of patients, allowing detailed statistical analysis before further conclusions can be drawn.

References

- [1] Dietz, V., Colombo, G., Jensen, L., Baumgartner, L.: Locomotor capacity of spinal cord in paraplegic patients. *Ann. Neurol.* 37, 574–582 (1995)
- [2] Dietz, V., Colombo, G., Jensen, L.: Locomotor activity in spinal man. *Lancet* 344, 1260–1263 (1994)
- [3] Werning, A., Muller, S.: Laufband locomotion with body weight support improved walking in persons with severe spinal cord injuries. *Paraplegia* 30, 229–238 (1992)
- [4] Nanassy, A., Cagol, E.: Laufband therapy based on rules of spinal locomotion is effective in spinal cord injured persons. *Eur. J. Neurosci.* 7, 823–829 (1995)
- [5] Colombo, G., Joerg, M., Schreier, R., Dietz, V.: Treadmill training of paraplegic patients using a robotic orthosis. *J. of Rehabilitation Research and Development* 37(6) (November/December 2000)
- [6] Hornby, T.G., Zemon, D.H., Campbell, D.: Robotic-assisted, body-weight-supported treadmill training in individuals following motor incomplete spinal cord injury. *Phys. Ther.* 85(1), 52–66 (2005)
- [7] Miyamoto, H., Israel, I., Mori, S., Sano, A., Sakurai, Y.: Approach to a powered orthosis for paralyzed lower limbs. In: *ICAR 1985*, pp. 451–458 (1985)
- [8] Kawamoto, H., Sankai, Y.: Power Assist System HAL-3 for Gait Disorder Person. *Phys. Ther.* 85(1), 52–66 (2005)
- [7] Miyamoto, H., Israel, I., Mori, S., Sano, A., Sakurai, Y.: Approach to a powered orthosis for paralyzed lower limbs. In: *ICAR 1985*, pp. 451–458 (1985)
- [8] Kawamoto, H., Sankai, Y.: Power Assist System HAL-3 for Gait Disorder Person. In: Miesenberger, K., Klaus, J., Zagler, W.L. (eds.) *ICCHP 2002. LNCS*, vol. 2398, p. 196. Springer, Heidelberg (2002)
- [9] Suzuki, K., Mito, G., Kawamoto, H., Hasegawa, Y., Sankai, Y.: Intention-based walking support for paraplegia patients with robot suit hal. *Advanced Robotics* 21(12), 383–408 (2007)
- [10] Yamawaki, K., Kawamoto, H., Nakata, Y., Eguchi, K., Sankai, Y., Ochiai, N.: Gait Training for a Spinal Cord Stenosis Patient using Robot Suit HAL[®] - A Case

Neurorehabilitation in Chronic Paraplegic Patients with the HAL[®] Exoskeleton – Preliminary Electrophysiological and fMRI Data of a Pilot Study

Matthias Sczesny-Kaiser^{1,*}, Oliver Höffken¹, Silke Lissek¹, Melanie Lenz¹, Lara Schlaffke¹, Volkmar Nicolas², Renate Meindl³, Mirko Aach³, Yoshiyuki Sankai⁴, Thomas A. Schildhauer³, Martin Tegenthoff¹, and Peter Schwenkreis^{1,*}

¹ Department of Neurology, BG University Hospital Bergmannsheil Bochum, Ruhr-University Bochum, Germany

{matthias.sczesny-kaiser, peter.schwenkreis}@rub.de

² Department of Radiology, BG University Hospital Bergmannsheil, Ruhr-University Bochum, Germany

volkmar.nicolas@rub.de
³ Department of General and Trauma Surgery, BG University Hospital Bergmannsheil, Ruhr-University Bochum, Germany

chirurgie@bergmannsheil.de

⁴ Cyberdyne Inc., Institute of Engineering Mechanics and Systems, University of Tsukuba, Japan

sankai@cyberdyne.jp

Abstract. Training leads to increased neuronal excitability, decreased inhibition and different types of neuronal plasticity. Most studies focus on cortical plastic changes after cerebral lesions or in healthy humans. In this study, we investigate cortical excitability and plastic changes after a three month period of HAL[®] exoskeleton supported treadmill training in patients with chronic incomplete spinal cord injury by means of electrophysiological measurements and functional magnetic resonance imaging. Here we report preliminary results of four patients.

1 Introduction

Recent studies have confirmed that regular treadmill training can improve walking capabilities in patients with incomplete spinal cord injury (SCI). In the last ten years, driven gait orthotics have been used in treadmill training to move the legs of patients in a physiological way. Now exoskeletons for paraplegic patients are available. In a pilot study, the exoskeleton HAL[®] (Cyberdyne, Japan) was used in treadmill training with bodyweight support. The HAL[®] system records voluntary electromyographic activity with surface electrodes from the extensor and flexor

* Corresponding authors.

muscles of hip and knee, and then actively supports the voluntarily initiated movements.

In the somatosensory and motor cortex of patients with SCI, large-scale somatotopic reorganization was demonstrated in a large number of studies [1-6]. For example, Henderson et al. investigated 20 subjects with complete thoracic SCI [7]. SCI resulted in significant primary somatosensory cortex (S1) reorganization, with the little finger representation moving medially towards the lower body representation. Furthermore, although SCI was associated with gray matter volume loss in the lower body representation, this loss was minimized as reorganization increased. As analyzed by diffusion tensor imaging, the authors postulated that S1 reorganization resulted from the growth of new lateral connections, and not simply from the unmasking of already existing lateral connections.

Considering these results, we hypothesized that treadmill training with the exoskeleton HAL[®] would lead to plastic changes in the primary somatosensory cortex of patients with incomplete chronic SCI as assessed by functional magnetic resonance imaging (fMRI). Moreover, plastic changes were expected to be a result of increased inhibition as assessed by somatosensory evoked potentials after paired-pulse stimulation of the median nerves.

Here we report preliminary results of the first four patients with chronic SCI, who participated in the HAL[®] training for a three-months-period.

2 Material and Methods

2.1 Subjects

We investigated four patients with chronic incomplete SCI with a time since injury of more than 6 months. One patient suffered from incomplete thoracic SCI, three patients from an incomplete lesion of the conus medullaris / cauda equina.

2.2 Electrophysiological Measurements

All patients underwent standard electrophysiological measurements with motor evoked potentials, somatosensory evoked potentials and nerve conduction studies before and after three months of training.

To assess changes of excitability of somatosensory cortex, we applied a paired-pulse electrical stimulation protocol to the median nerves while recording SEPs from the right and left S1, respectively. The stimulation protocol consisted of a single pulse (pulse duration 0.2 ms) followed by a paired pulse (pulse duration 0.2 ms, ISI 30 ms) delivered transcutaneously via a block stimulator located above the median nerve at the wrist at a frequency of 3 Hz. Stimulation intensity was 2.5 times of each patient's individual sensory threshold and was accompanied in all patients by a small muscular twitch in the thenar muscles.

SEPs were recorded using an electrode over the left and right S1, located 2 cm posterior to C3 and C4 (CP3 and CP4) according to the International 10–20 system. A reference electrode was placed over midfront (Fz) position. SEPs were recorded in epochs from 20 ms before to 200 ms after stimulus onset with a 32-channel amplifier (bandpass filter, 100–2000 Hz; Brain AMP MR; Brain Products) and stored for off-line analysis. For each single- and paired-pulse stimulation, 800 stimulus-related epochs were recorded. Peak-to-peak amplitudes of the cortical N20–P25 SEP components were analyzed. Paired-pulse suppression was expressed as a ratio ($A2s/A1$) of the amplitudes of the subtracted second ($A2s$) and the first ($A1$) N20–P25 peaks. Amplitude ratios < 1 indicate paired-pulse-suppression while ratios > 1 represent paired-pulse facilitation.

2.3 Functional MRI Scan

fMRI studies were conducted in a 3 Tesla scanner using a 32-channel head coil (Achieva 3.0T X, Philips Healthcare). Blood-oxygen level-dependent (BOLD) images were obtained with a SpinEcho EPI sequence (TR 3200 ms, TE 35 ms, 224 mm “field of view”, 3 mm slice thickness, voxel $2 \times 2 \times 3$ mm). During the scan, tactile stimuli were delivered simultaneously to the three phalanges of the second digit of both hands using an airpuff device. A total of 480 stimuli were applied to each side at a frequency of 1.25 Hz. Preprocessing and analysis of the event-related fMRI data were performed using SPM8 (Wellcome Trust Center for Neuroimaging, University College London, UK). Functional imaging data were corrected for slice-timing and head motion.

2.4 Treadmill Training with HAL®

All patients performed daily treadmill training with the exoskeleton HAL® (Cyberdyne, Japan) and body weight support for a three month period. Training was supervised by a physiotherapist and a medical doctor.

3 Results

After three months of training, which led to a significant functional improvement in all patients (results are presented separately at this conference), we found an increased paired-pulse inhibition of somatosensory evoked potentials in both hemispheres following median nerve stimulation at the wrist (as shown in Fig. 1). This increased inhibition was accompanied by a reduced S1 activation of the activated area in both hemispheres after tactile stimulation of the index finger (as shown in Fig. 2). Standard electrophysiological measurements did not differ between pre- and post-conditions (not shown).

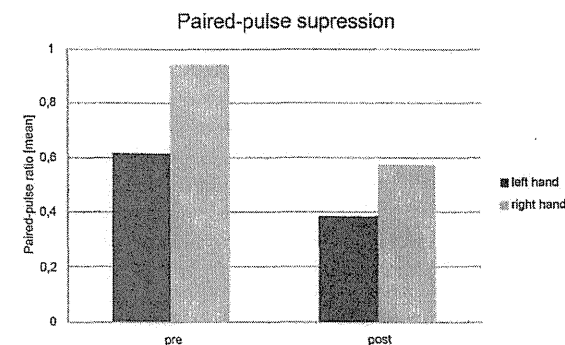


Fig. 1 Mean paired-pulse ratios are plotted for both hemispheres contralateral to the stimulated hand. After exoskeleton training period (post), the patients show decreased amplitude ratios compared with the baseline (pre).

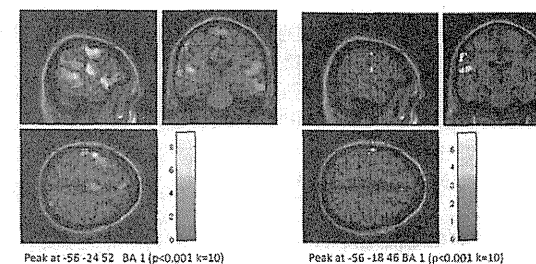


Fig. 2 Functional magnetic imaging data of one patient show a decreased activation in the somatosensory cortex during tactile stimulation after exoskeleton HAL® training.

4 Discussion

These preliminary results show plastic changes in the brain, which accompany the functional improvement in these four patients. Since standard electrophysiological parameters (MEP, SEP, nerve conduction studies) did not change after three months of training, the results suggest that cortical plastic changes due to improved use of the remaining intact spinal connections, rather than regeneration of the lesioned spinal connections might be responsible for the functional improvement in these patients.

5 Conclusion

Treadmill training using the exoskeleton HAL® seems to be a useful innovative training method for chronic paraplegic SCI patients. However, so far these